Kobe University Repository : Kernel

PDF issue: 2025-12-05

Reduced nucleotomy-induced intervertebral disc disruption through spontaneous spheroid formation by the Low Adhesive Scaffold Collagen (LASCol)

Takeoka, Yoshiki ; Yurube, Takashi ; Morimoto, Koichi ; Kunii, Saori ; Kanda, Yutaro ; Tsujimoto, Ryu ; Kawakami, Yohei ; Fukase, Naomasa ;…

(Citation)
Biomaterials,235:119781-119781

(Issue Date)
2020-03

(Resource Type)
journal article

(Version)
Version of Record

(Rights)
© 2020 The Authors. Published by Elsevier Ltd.
This is an open access article under the CC BY license
(http://creativecommons.org/licenses/by/4.0/).

(URL)
https://hdl.handle.net/20.500.14094/90006944

Biomaterials 235 (2020) 119781

Contents lists available at ScienceDirect

Biomaterials

journal homepage: www.elsevier.com/locate/biomaterials

Reduced nucleotomy-induced intervertebral disc disruption through spontaneous spheroid formation by the Low Adhesive Scaffold Collagen (LASCol)

Yoshiki Takeoka[a], Takashi Yurube[a,*], Koichi Morimoto[b], Saori Kunii[b], Yutaro Kanda[a], Ryu Tsujimoto[a], Yohei Kawakami[a], Naomasa Fukase[a], Toshiyuki Takemori[a], Kaoru Omae[c], Yuji Kakiuchi[a], Shingo Miyazaki[a], Kenichiro Kakutani[a], Toru Takada[a], Kotaro Nishida[a], Masanori Fukushima[c], Ryosuke Kuroda[a]

[a] Department of Orthopaedic Surgery, Kobe University Graduate School of Medicine, 7-5-1 Kusunoki-cho, Chuo-ku, Kobe, 650-0017, Japan
[b] Department of Genetic Engineering, Faculty of Biology-Oriented Science and Technology, Kindai University, 930 Nishimitani, Kinokawa, Wakayama, 649-6493, Japan
[c] Translational Research Center for Medical Innovation (TRI), Foundation for Biomedical Research and Innovation at Kobe, 1-5-4 Minatojima-Minamimachi, Kobe, 650-0047, Japan

ARTICLE INFO

Keywords:
Low Adhesive scaffold Collagen (LASCol)
Atelocollagen (AC)
Biodegradable scaffold for tissue-engineering regeneration
Intervertebral disc degeneration and herniation
Rat tail nucleotomy model of disc disruption
Spine

ABSTRACT

Back pain is a global health problem with a high morbidity and socioeconomic burden. Intervertebral disc herniation and degeneration are its primary cause, further associated with neurological radiculopathy, myelopathy, and paralysis. The current surgical treatment is principally discectomy, resulting in the loss of spinal movement and shock absorption. Therefore, the development of disc regenerative therapies is essential. Here we show reduced disc damage by a new collagen type I-based scaffold through actinidain hydrolysis—Low Adhesive Scaffold Collagen (LASCol)—with a high 3D spheroid-forming capability, water-solubility, and biodegradability and low antigenicity. In human disc nucleus pulposus and annulus fibrosus cells surgically obtained, time-dependent spheroid formation with increased expression of phenotypic markers and matrix components was observed on LASCol but not atelocollagen (AC). In a rat tail nucleotomy model, LASCol-injected and AC-injected discs presented relatively similar radiographic and MRI damage control; however, LASCol, distinct from AC, decelerated histological disc disruption, showing collagen type I-comprising LASCol degradation, aggrecan-positive and collagen type II-positive endogenous cell migration, and M1-polarized and also M2-polarized macrophage infiltration. Reduced nucleotomy-induced disc disruption through spontaneous spheroid formation by LASCol warrants further investigations of whether it may be an effective treatment without stem cells and/or growth factors for intervertebral disc disease.

1. Introduction

Back pain increases with age, affects 70–85% of people during their lives, and causes disability [1] with estimated healthcare costs up to $100 billion/year in the US [2]. The cause of back pain is multifactorial; however, intervertebral disc degeneration is one of the independent risk factors [3]. Intervertebral disc herniation, an injury with degenerative wear and tear, occurs even in the youth, limits daily and sports activities, and requires surgery in 10% [4].

The intervertebral disc has a complex structure with the nucleus pulposus (NP) encapsulated by the annulus fibrosus (AF) and endplates [5]. The collagenous, laminar AF surrounds the central, gelatinous NP, maintaining pressurization of the NP for support of compressive loading and facilitation of multidimensional spinal movement [5]. While the AF comes from the mesenchyme [6], the origin of the NP is the notochord [7]. Disc cells, positive for brachyury, CD24 (both disc NP markers) [8],

* Corresponding author.
E-mail addresses: yoshiki_tkk@hotmail.com (Y. Takeoka), takayuru-0215@umin.ac.jp (T. Yurube), morimoto@waka.kindai.ac.jp (K. Morimoto), skunii@waka.kindai.ac.jp (S. Kunii), ykanda221@gmail.com (Y. Kanda), tsujiryu1105@yahoo.co.jp (R. Tsujimoto), yohei_kawakami@hotmail.com (Y. Kawakami), nfukase@msn.com (N. Fukase), westlife_take@yahoo.co.jp (T. Takemori), k-omae@tri-kobe.org (K. Omae), yuji_uz_7@yahoo.co.jp (Y. Kakiuchi), mghff229@yahoo.co.jp (S. Miyazaki), kakutani@med.kobe-u.ac.jp (K. Kakutani), takada-t@hokuto-hp.or.jp (T. Takada), kotaro@med.kobe-u.ac.jp (K. Nishida), mfukushi@tri-kobe.org (M. Fukushima), kurodar@med.kobe-u.ac.jp (R. Kuroda).

https://doi.org/10.1016/j.biomaterials.2020.119781
Received 29 July 2019; Received in revised form 8 January 2020; Accepted 10 January 2020
Available online 11 January 2020
0142-9612/ © 2020 The Authors. Published by Elsevier Ltd. This is an open access article under the CC BY license (http://creativecommons.org/licenses/BY/4.0/).

tyrosine kinase with Ig and EGF homology domains 2 (Tie2) (disc NP progenitor marker) [9], collagen type V alpha 1 [10], and CD146 (both disc AF markers) [11], have a chondrocytic phenotype to produce matrix components comprising proteoglycans (principally aggrecan) and collagens (primarily types I in the AF and II in the NP) [12]. Furthermore, the disc is an immune-privileged, the largest avascular organ in the body [13]. Disc cells thus live under an extremely harsh environment—low glucose, oxygen, and pH and high osmolality and load fluctuation [14]. While age-related disc changes characterized by the loss of notochordal cells appear from early childhood as observed in people aged 11–16 years [15], ~40% of people aged under 30 years and 90% of those aged over 55 years present structural lumbar disc degeneration [16], which can cause back pain [17].

Herniated and degenerated discs can present not only back pain but also radicular pain, numbness, muscle weakness, and then paralysis in the worst scenario [18]. Despite successful conservative treatment outcomes with medication and physiotherapy in disc disease, non-responders reluctantly require surgery [4]. Surgical interventions predominantly include the excision of damaged discs, resulting in the function loss, immobilization, and potential additional complications due to the altered biomechanics [19]. Therefore, the development of new therapies for direct disc repair is an urgent issue.

Stem cells [20], growth factors [21], and tissue engineering [22] have been applied for disc regeneration. Each trial is effective; nevertheless, unclarified aspects still remain for the human body application. Mesenchymal stem cells are at risk of osteophyte [23] and also neoplasm [24] formation with an extremely low survival rate of intradiscally transplanted cells [20]. The bone morphogenetic protein-2 is associated with carcinogenesis [25]. Hence, interest has recently expanded to bioengineering approaches that exploit endogenous cell populations to restore the disc structure and function [22]. Injectable scaffolds using atelocollagen (AC), alginate, hyaluronan, and chitosan have been tested [26]. As a collagen-based scaffold, AC has often been used clinically, such as autologous chondrocyte-seeded AC for cartilage repair [27] and porous hydroxyapatite/AC composites for bone defect [28]. While several kinds of scaffold have shown the regenerative potential, no scaffolds are clinically available for disc treatment because of the undiscovered repair mechanisms as well as safety concerns [22].

In the tissue-engineering field, spheroid formation has increased attention because of its 3D cell-culturing structure capable of mimicking the *in-vivo* environment [29]. Morphological characteristics, metabolic activity, and function of cells are better maintained in 3D than 2D [29]. Spheroid formation is effective in maintaining the phenotype of progenitor cells in the disc [9]. We thus developed a new collagen-based scaffold through the hydrolysis with actinidain protease, which was named as the Low Adhesive Scaffold Collagen (LASCol) from the characteristic of its high 3D spheroid-forming capability [30–32]. The LASCol is designed by removing major parts of the N-terminal and C-terminal telopeptides of collagen type I, while AC is similarly obtained from collagen type I by partially eliminating the terminal telopeptides [30,32]. In scanning electron microscopy, LASCol has weaker fibril formation than AC just after the preparation; however, the microstructure of both gels become similar approximately 6 h later [30,31] (Fig. 1A). As the terminal telopeptides are antigenic, AC is relatively low-immunogenic whereas LASCol is considered further safe. The LASCol has additional advantages with a higher water-solubility providing wide ranges of concentration and mechanical strength, increased sensitivity to changes in temperature contributing to rapid stabilization, and faster degradability than AC (Fig. 1B). These characteristics satisfy requirements for an injectable scaffold. Therefore, we hypothesized that LASCol could repair damaged intervertebral disc tissues by inducing endogenous cell migration and altering matrix turnover through spontaneous spheroid formation even in the severe surroundings for cell survival [13,14,29]. Our strategies for the clinical use of LASCol are the prevention of degeneration after discectomy in young patients with herniated discs and also the delayed progression of age-related degeneration in middle to old patients with symptomatic degenerative discs. The injectable and relatively safe characteristics of LASCol could enable the percutaneous administration as well as the direct intraoperative supplementation, aiming the preventive application of LASCol for herniated and degenerative disc disease in the future. Our objective was to elucidate the mechanisms and potential of LASCol and mediated spheroid formation for disc damage reduction by the scaffold only in a rat tail nucleotomy-induced disc disruption model *in vivo* and in human clinical samples surgically obtained *in vitro*.

2. Materials and methods

2.1. Ethics statement

All human and animal experiments were performed under the approval and guidance of the Institutional Review Board (160004) and Institutional Animal Care and Use Committee (P161105) at Kobe University Graduate School of Medicine. Written informed consent was obtained from each patient in accordance with the principles of the Declaration of Helsinki and the laws and regulations of Japan.

2.2. Antibodies and reagents

The antibodies and reagents used are listed in Supplementary Table 1.

2.3. Materials

The LASCol was developed from porcine skin-derived collagen type I by actinidain hydrolysis [30–32] (Fig. 1A). To assess immunogenic potential of LASCol, an antigen-stimulation test was performed at Japan Food Research Laboratories (Tokyo, Japan) (No. 15065266001–0101). Briefly, intraperitoneal LASCol injection was conducted for guinea pigs at 1, 3, and 5 d, and intravenous LASCol injection was conducted at 15 and 22 d for stimulation ($n = 4$). As a control, horse serum was injected in the same manners ($n = 4$). No allergic response was all found in the LASCol group, while dyspnea was observed in all, 3 of which were dead in the control group. This test indicates a safe, relatively low antigenicity of LASCol. A low-immunogenic potential of LASCol makes it possible to apply directly without any immunosuppression even in xenogeneic transplantation.

In vitro, 7.0-mg/ml LASCol gel, consisting of Dulbecco's modified Eagle's culture solution, Reconstitution buffer, and 10.0-mg/ml LASCol solution from 5.0-mM hydrochloric acid and freeze-dried LASCol, was distributed at 1 ml in a 35-mm dish or each well of a 6-well plate and at 200 μm in each well of a 24-well plate at 37 °C overnight. Similarly, 2.1-mg/ml AC gel, consisting of 3.0-mg/ml AC solution, was distributed at the same amounts.

In vivo, 42.0-mg/ml, 21.0-mg/ml, 14.0-mg/ml, and 7.0-mg/ml LASCol and 7.0-mg/ml AC gels were prepared from saline, Reconstitution buffer, and LASCol or AC solution. Based on the difference in solubility between LASCol and AC, 21.0-mg/ml LASCol and 7.0-mg/ml AC gels were compared. Effects of LASCol were also tested at other concentrations. Both gels had an injectable, low viscosity on ice and became stabilized at the body temperature of 37 °C within 1 min after the intradiscal injection, the storage modulus of which at 37 °C after 30 min was approximately ≥1.4 kPa, within a reported range in the viscosity of *in-vivo* disc NP tissues [33]. The LASCol gel becomes cloudy compared to the AC gel, which resulted from the difference in fibrosity (Fig. 1B).

2.4. Cells

Human disc NP and AF cells were isolated from patient specimens undertaking lumbar discectomy or interbody fusion surgery ($n = 15$ for NP: age, 39.2 ± 17.1 [16–76] years; sex, 10 males and 5 females;

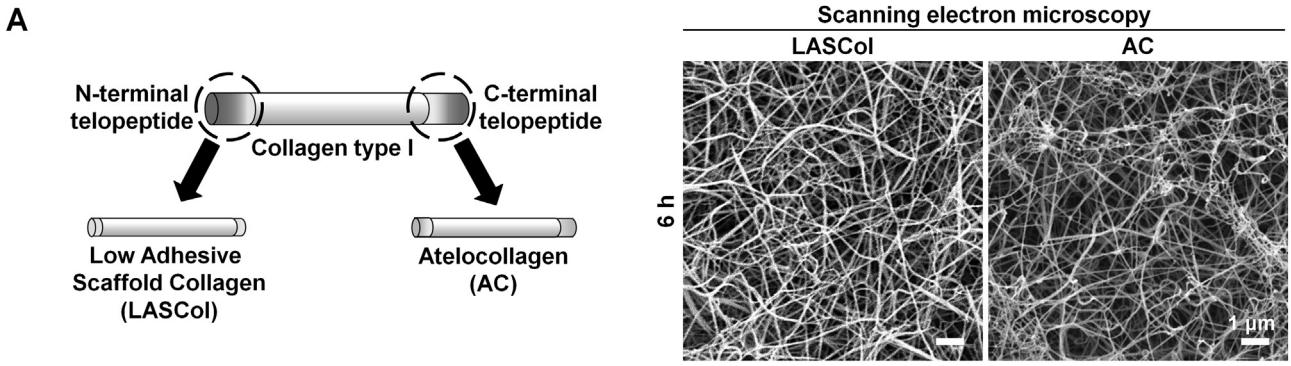

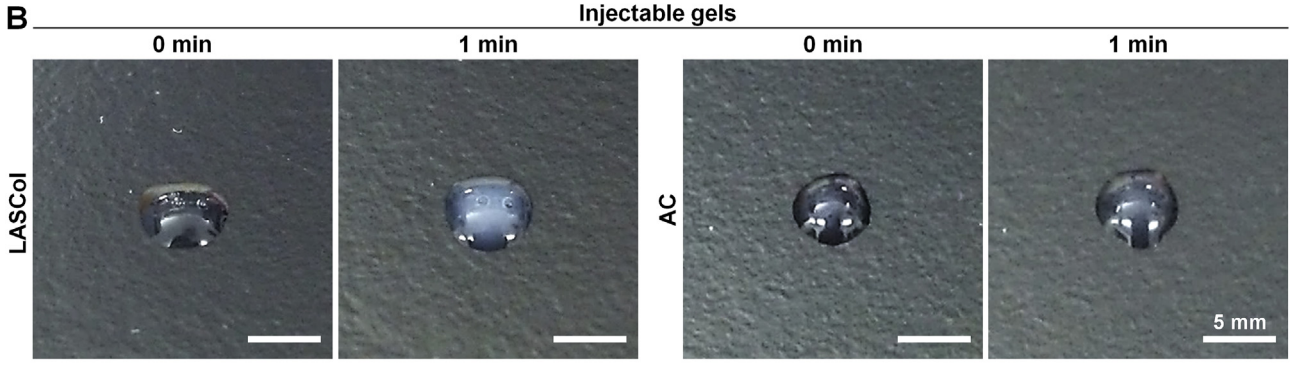

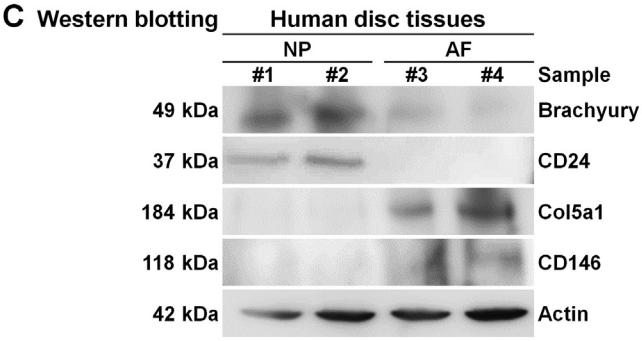

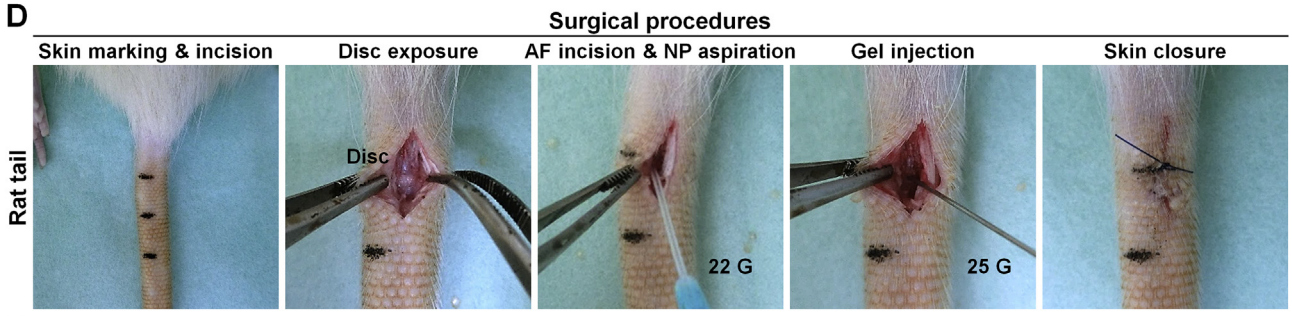

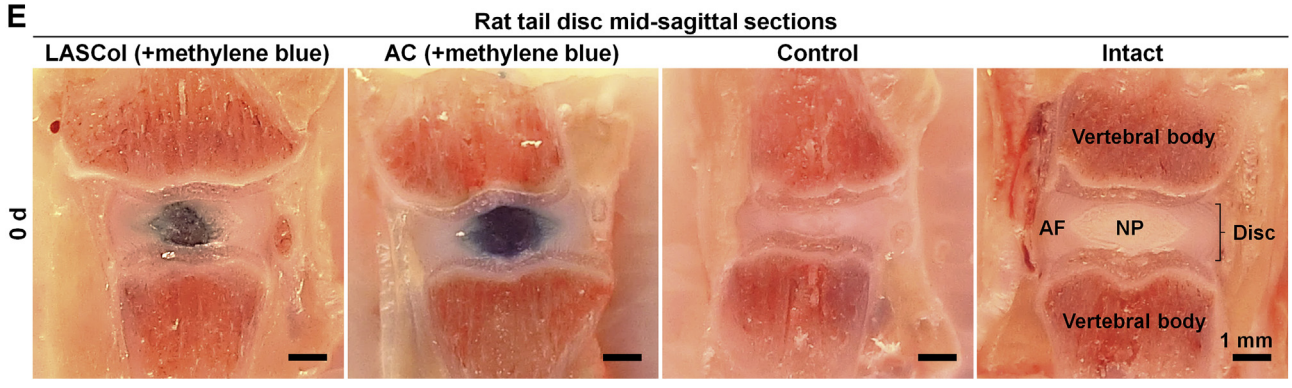

(caption on next page)

Fig. 1. Characteristics of LASCol, surgical procedures, and confirmation of disc cell phenotypes. (A) Schematic illustration of the LASCol microstructure. The LASCol is developed by removing major parts of the N-terminal and C-terminal telopeptides of collagen type I, while AC is similarly obtained from collagen type I by partially eliminating the terminal telopeptides. In scanning electron microscopy, LASCol has weaker fibril formation than AC just after the preparation; however, the microstructure of both gels become similar approximately 6 h later. (B) Macroscopic appearances of injectable LASCol (21.0 mg/ml) and AC (7.0 mg/ml) gels. Both gels were prepared to have an injectable, low viscosity on ice and become stabilized at 37 ˚C for 1 min. The difference in solubility between LASCol and AC resulted in different gel concentrations. The LASCol gel becomes cloudy compared to the AC gel, which resulted from the difference in fibrosity. (C) Validation of surgical disc NP-tissue and AF-tissue acquisition. Western blotting for disc NP-phenotypic brachyury and CD24 and AF-phenotypic collagen type V alpha 1 and CD146 was performed in total protein extracts from human disc NP and AF tissues of patients who underwent lumbar spine surgery. Actin was used as a loading control. (D) Surgical procedures in a rat tail nucleotomy model. Under general anesthesia, 12-week-old male Sprague–Dawley rats underwent nucleotomy by disc AF incision and NP aspiration with a 22-gauge catheter through a 1-cm longitudinal incision. Subsequently, LASCol gel (7.0–42.0 mg/ml), AC gel (7.0 mg/ml), or solvent as the control was injected at 15 μl into the disc using a 25-gauge catheter. (E) Macroscopic appearances of rat tail LASCol-injected (21.0 mg/ml), AC-injected (7.0 mg/ml), solvent control, and untreated intact disc mid-sagittal sections. Successful intradiscal gel injection without extrusion was confirmed by using a methylene blue dye. (For interpretation of the references to color in this figure legend, the reader is referred to the Web version of this article.)

Pfirrmann degeneration grade [34], median 2 ± 0.6 [2–4]) (n = 12 for AF: age, 61.8 ± 11.6 [41–80] years; sex, 9 males and 3 females; Pfirrmann degeneration grade, median 3 ± 0.5 [2–4]). We carefully obtained disc AF tissues by box-cutting AF sharply by a scalpel and NP tissues from the first bite of tissues by a laminectomy rongeur without any violation of vertebral endplates, both of which were collected from discarded surgical waste. Immediately after surgery, disc NP and AF tissues were digested for cell isolation in Dulbecco's modified Eagle's medium (DMEM) with 10% fetal bovine serum (FBS), 1% penicillin/streptomycin, and 0.114% collagenase type 2 at 37 ˚C for 1 h in the NP and 12 h in the AF. Isolated cells were grown in 1% penicillin/streptomycin-supplemented DMEM with 10% FBS. To retain the phenotype, only first-passage cells were used for cell-counting (n = 6), immunofluorescent (n = 6), and real-time reverse transcription–polymerase chain reaction (RT–PCR) (n = 3) experiments following 72-h pre-culture. Cell samples collected abundantly were used across experiments. Experimental conditions were maintained throughout at 37 ˚C under 5% CO_2, 2% O_2 to stimulate the physiologically hypoxic disc environment [13,14].

The acquisition of human disc specimens specific for the NP and AF was validated by Western blotting using directly extracted proteins from residual tissues as described previously [35,36]. Briefly, tissues were homogenized using the MS-100R bead-beating disrupter for 30 s twice at 4 ˚C in the T-PER tissue protein extraction reagent with protease and phosphatase inhibitors. Soluble proteins were collected after centrifugation at 20,000 g for 15 min at 4 ˚C. Protein concentration was determined by the bicinchoninic acid assay. Equal 30-mg amounts of protein were mixed with the electrophoresis sample buffer and boiled for 5 min before loading onto a 7.5–15.0% polyacrylamide gel. Separated tissue proteins in the Tris–glycine–sodium dodecyl sulfate buffer system were transblotted electrically and probed with primary antibodies (1:200–1:1000 dilution) for brachyury [8] and CD24 [8] (disc NP markers), collagen type V alpha 1 [10] and CD146 [11] (disc AF markers), and actin (loading control) for 12 h in 4 ˚C followed by secondary antibodies (1:2000 dilution). Signals were visualized by enhanced chemiluminescence. Images were obtained using the Chemilumino analyzer LAS-3000 mini. Consequently, an acceptable disc NP-specific and AF-specific marker expression was confirmed (Fig. 1C).

2.5. Animals

Twelve-week-old male Sprague–Dawley rats were used. Under general anesthesia, 1-cm longitudinal incision was made along the tail to expose the lateral portion of the caudal (C) disc. A #11 scalpel blade was inserted 1.5 mm into the disc. Nucleotomy by disc AF incision and NP aspiration with a 22-gauge catheter on a 5-ml syringe was conducted as described previously [37,38] (Fig. 1D).

Nucleotomy at C8–C9, C9–C10, and C10–C11 was performed to assess effects of materials in 44 rats (weight 427.1 ± 15.2 [405–450] g). Intradiscal 15-μl injection of 21.0-mg/ml LASCol gel, 7.0-mg/ml AC gel, and solvent control (saline and Reconstitution buffer) was conducted using a 25-gauge catheter, respectively. These three treatments were all applied in each rat tail to eliminate the individual difference and randomly at each disc segment. The injection volume was determined based on prior evidence [39]. Intradiscal gel injection without extrusion was preliminarily established by using a methylene blue dye (Fig. 1E). Radiographs were taken before and 7–56 d after surgery (n = 8). Then, magnetic resonance images (MRIs) were taken 28 d after surgery (n = 6). After imaging, vertebral body–disc–vertebral body functional spinal units were frozen with Super Cryoembedding medium quickly in liquid nitrogen. Mid-sagittal sections at 5-μm thickness were prepared for histology as described previously [40]. Histomorphological Safranin-O staining and immunofluorescence were performed at postoperative 0–56 d (both n = 6).

Nucleotomy at C8–C9, C9–C10, C10–C11, and C11–C12 was performed to assess dose-dependent effects of LASCol in 24 rats (weight 436.9 ± 17.8 [415–463] g). Intradiscal 15-μl injection of 42.0-mg/ml, 21.0-mg/ml, 14.0-mg/ml, and 7.0-mg/ml LASCol gels was conducted, respectively. These four concentrations were all applied in each rat tail to exclude the individual difference and randomly at each disc segment. Radiographs were taken before and 7–56 d after surgery (n = 6).

2.6. Immunofluorescence

In vitro, in a 35-mm dish coated with 1-ml LASCol or AC gel, 3.0×10^5 human disc NP and AF cells/well were cultured in 2-ml 10% FBS-supplemented DMEM for 120 h. Fresh media of 500 μl were gently added at 72 h without exchange to prevent cell detachment. Cells were fixed in 4% paraformaldehyde for 30 min. To assess the phenotype, disc NP cells were stained with 1:100-diluted primary antibodies for brachyury (disc NP marker) [8], Tie2 (disc NP progenitor marker) [9], and aggrecan (disc matrix component) [12] or for brachyury, collagen type I (LASCol constituent) [12,30,32], and collagen type II (disc NP matrix component) [12] overnight at 4 ˚C, followed by 1:400-diluted Alexa Fluor® 488, 568, and 647 secondary antibodies for 1 h at room temperature. Similarly, collagen type V alpha 1 [10], CD146 [11] (both disc AF markers), and collagen type I (LASCol constituent and disc AF matrix component) or aggrecan primary antibodies and Alexa Fluor® 488, 568, and 647 secondary antibodies were used for disc AF-cell staining. The 4′,6-diamidino-2-phenylindole (DAPI) was used for counterstaining. Images were photographed by the BZ-X700 microscope. The number of positive cells was counted in five random low-power fields (× 100) using the ImageJ software (https://imagej.nih.gov/ij/). Briefly, we created binary images at a fixed intensity level and counted positive cells included in the field. The positive cell percentage for brachyury, Tie2, aggrecan, and collagen types I and II in the NP and for collagen type V alpha 1, CD146, collagen type I, and aggrecan in the AF was calculated as relative to the total number of DAPI-positive cells.

In vivo, rat caudal disc sections were fixed with 4% paraformaldehyde for 30 min, decalcified in 10% ethylenediaminetetraacetic acid for 30 min, antigen-retrieval, permeabilized, and blocked. Multi-color immunofluorescence was performed with 1:200-diluted primary antibodies overnight at 4 ˚C for collagen types I and II to assess the composition of matrix [12] and scaffolds [30,32], for brachyury [8], Tie2

[9], and aggrecan [12] to assess the phenotype of cells, or for ionized calcium binding adaptor molecule 1 (Iba1, pan-macrophage marker) [41], CD86 (M1-polarized macrophage marker, characterized by producing pro-inflammatory mediators) [42], and CD163 (M2-polarized macrophage marker, characterized by responses to anti-inflammation and tissue remodeling) [43] to assess the infiltration of macrophages, followed by 1:400-diluted Alexa Fluor® 488, 568, and 647 secondary antibodies for 1 h at room temperature. The DAPI was used for counterstaining. Similarly, imaging and positive cell-counting were performed by creating binary images at a fixed level with ImageJ, and the percentage of positive cells for brachyury, Tie2, aggrecan, Iba1, CD86, and CD163 in the NP was calculated.

2.7. Time-lapse cell-counting and spheroid-counting

In vitro, in a 24-well plate coated with 200-μl LASCol or AC gel, 2.0×10^4 human disc NP and AF cells/well were cultured in 500-μl 10% FBS-supplemented DMEM. Fresh media of 100 μl were gently added every 72 h without exchange. Time-lapse photographing was performed every 6 h for 192 h. The number of cells and spheroids was counted in five random low-power fields (× 100) using ImageJ. In this study, spheroid was defined as the aggregation of ≥3 cells.

2.8. RNA isolation and real-time RT–PCR

In vitro, in a 6-well plate coated with 1-ml LASCol or AC gel compared to the non-coated condition, 2.0×10^5 human disc NP cells/well were cultured in 2-ml 10% FBS-supplemented DMEM for 168 h. Fresh media of 500 μl were gently added every 72 h without exchange. At 72 and 168 h, total RNA was extracted using the RNeasy mini kit, and 0.1-μg RNA was reverse-transcribed with random primers. Messenger RNA (mRNA) expression levels of chondrogenic *SOX9* encoding SRY-box 9 (chondrogenesis regulator) [44], *COMP* encoding cartilage oligomeric matrix protein (cartilage turnover marker) [45], and *TGFB1* encoding transforming growth factor beta 1 (chondrogenesis inducer) [46] relative to *ATP synthase, H+ transporting, mitochondrial F0 complex, subunit B1* (*ATP5F1*) [47] as an endogenous control were assessed in duplicate by real-time RT–PCR using a SYBR Green fluorescent dye. These target genes were chosen to analyze the trend of cartilage differentiation. To identify appropriate housekeeping genes for references, mRNA expression levels of 15 genes were evaluated using a human housekeeping gene primer set, and *ATP5F1* was selected as a reference based on the highest stability in mRNA expression regardless of complementary DNA concentration. The commercialized, validated primer sequences were used as follows: *SOX9*, forward 5′-GGAGATGAAATCT GTTCTGGGAATG-3′, reverse 5′-TTGAAGGTTAACTGCTGGTGTTCTG-3'; *COMP*, forward 5′-AGGGTACCCAACTCAGACCAGAAG-3′, reverse 5′-TGTTAGGCACCGTGGGACAG-3'; *TGFB1*, forward 5′-TCCTGGCGAT ACCTCAGCAA-3′, reverse 5′-GCTAAGGCGAAAGCCCTCAA-3'; *ATP5F1*, forward 5′-GAAGCAGGCTTCCATCCAACA-3′, reverse 5′-TCGTTCCCGG TAAGTAACTTCCAA-3'. Measurements were performed using the Thermal Cycler Dice® Real Time System Single PCR system. Melting curve analysis was performed using the Dissociation Curve software to ensure that only a single product was amplified. Relative mRNA expression was analyzed using the $2^{-\Delta\Delta Ct}$ method [48]. The value of non-coated control sample was set as 1.

2.9. Radiography

In vivo, lateral radiographs were taken using VPX-30E system and IXFR film (exposure time 40 s; distance 40 cm; current 3 mA; voltage 35 kV). Radiographs were measured twice at one-week intervals by each of two investigators blinded to the study purpose. Disc height was measured using ImageJ, normalized to adjacent vertebral body heights as the disc height index (DHI), shown as the percent of preoperative DHI (%DHI = [postoperative DHI/preoperative DHI] × 100) as described previously [49], and further normalized to the intact disc as the normalized %DHI (normalized %DHI = [experimental %DHI/intact %DHI] × 100) [50] (Fig. 4A).

2.10. MRI

In vivo, MRIs were taken using 4.7-T Varian Unity Inova 200 MHz MRI unit. Sagittal T2-weighted imaging and T2 mapping (repetition time/echo time 2000/30 and 60 ms [2 echoes], field of view 100 × 50 mm, slice thickness 2 mm, matrix size 512 × 512 mm, number of experiments 4, acquisition time 35 min) were performed. Region of interest was positioned in the disc center using the MATLAB software 9.1.0.441655 (R2016b), and mean T2 values were computed within the region as described previously [51].

2.11. Safranin-O staining

In vivo, safranin-O, fast green, and hematoxylin staining was performed to demonstrate proteoglycan distribution. Disc NP-cell number and safranin-O-positive area were measured using ImageJ. Briefly, we created binary images at a fixed intensity level and measured the area between vertebral endplates. We counted cells included in the area.

2.12. Statistical analysis

Data are expressed as the mean ± standard deviation in the text and box plots in the graphs. The Student t-test was used to assess effects of LASCol and AC *treatments* in *in-vitro* immunofluorescence. One-way analysis of variance (ANOVA) with the Tukey–Kramer post-hoc test was used to assess effects of multiple *treatments* in *in-vivo* MRI. Two-way repeated measures ANOVA with the Tukey–Kramer post-hoc test was used to assess effects of *treatment* and *time* in *in-vitro* cell-counting and spheroid-counting and *in-vivo* radiography, histomorphology, and immunofluorescence (experiments using replicates from the same donors) as well as in *in-vitro* real-time RT–PCR (target gene expression analysis shown as relative values of the control). In addition, intra-class correlation coefficient was calculated to determine intra-observer and inter-observer reliabilities for the measurement of radiographic parameters. The *P*-values of < 0.05 were regarded as statistically significant using IBM SPSS Statistics 23.0 (IBM, Armonk, NY).

3. Results

3.1. Spontaneous spheroid formation of human disc NP and AF cells on LASCol

First, we observed spheroid formation of human disc NP and AF cells on the LASCol gel *in vitro*. Both cell types proliferated in monolayer on the AC gel but demonstrated spheroid formation on the LASCol gel (Fig. 2A). Time-lapse photographing presented cell-aggregating spheroid formation on the LASCol gel only, the pattern of which was similar between disc NP and AF cells (Fig. 2B). Cell-counting analysis found no apparent increases in disc NP and AF cells on the LASCol but not AC gel ($P < 0.001$) (Fig. 2C). However, the number of spheroids, defined as ≥3 cell aggregation, progressively increased in both cells on the LASCol gel only ($P < 0.001$) (Fig. 2D). Spontaneous spheroid formation of disc NP and AF cells on the LASCol gel indicates a high compatibility of LASCol with both cell types.

3.2. Enhanced disc-cell and chondrocyte phenotype of human disc NP and AF cells on LASCol

Next, we assessed effectiveness of spheroid formation in human disc NP and AF cells on the LASCol gel *in vitro*. In disc NP cells, multi-color immunofluorescence showed elevated expression of brachyury (disc NP marker) [8], Tie2 (disc NP progenitor marker) [9], and aggrecan (disc

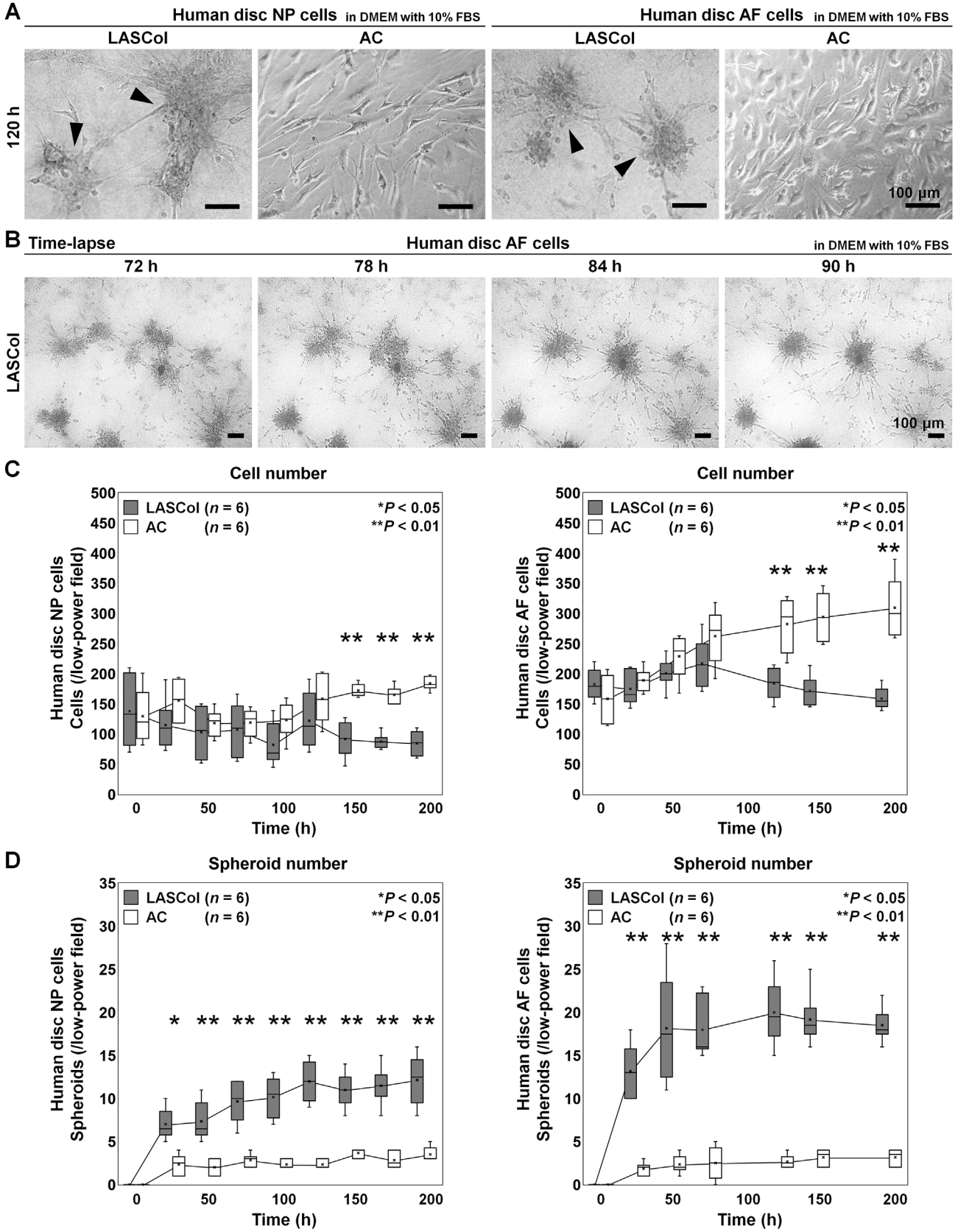

Fig. 2. Spontaneous spheroid formation of human disc NP and AF cells on LASCol. (A) Human disc NP and AF cells cultured on the LASCol or AC gel in 10% FBS-supplemented DMEM at 120 h. Black triangles indicate spheroids. (B) Time-lapse human disc AF cells cultured on the LASCol gel in 10% FBS-supplemented DMEM at 72–90 h. (C) Changes in the number of human disc NP and AF cells cultured on the LASCol or AC gel. (D) Changes in the number of human disc NP and AF spheroids cultured on the LASCol or AC gel. The spheroid was defined as the aggregation of ≥3 cells. In (C) and (D), the number of cells and spheroids was counted in five random low-power fields (× 100). Data are presented with box plots ($n = 6$). Two-way repeated measures ANOVA with the Tukey–Kramer post-hoc test was used.

matrix component) [12] in spheroids on the LASCol gel compared to on the AC gel (brachyury, $P < 0.001$; Tie2, $P < 0.001$; aggrecan, $P = 0.001$). In addition, expression of collagen type II (disc NP matrix component) [12] increased in spheroids on the LASCol gel compared to on the AC gel, while collagen type I (LASCol constituent) [12,30,32] was comparable between on the LASCol and AC gels (collagen type II, $P = 0.004$; collagen type I, $P = 0.39$) (Fig. 3AC). In disc AF cells, collagen type V alpha 1 [10] and CD146 (both disc AF markers) [11] were more abundant in spheroids on the LASCol gel than on the AC gel (collagen type V alpha 1, $P = 0.02$; CD146, $P < 0.001$). Immunopositivity for aggrecan appeared to be higher on LASCol than on AC, showing the tendency toward increase on the LASCol gel although it did not reach statistical significance ($P = 0.06$) (Fig. 3BC). Meanwhile, the percentage of immunopositive cells for collagen type I (disc AF matrix component) [12] was similarly high between on LASCol and AC, despite marked collagen type I expression in spheroids on the LASCol gel than on the AC gel ($P = 0.20$) (Fig. 3BC). A high level of background signals detected in all measurements for collagen type I in disc NP and AF cells on LASCol and AC gels would indicate the presence of collagen type I-comprising LASCol and AC gels. Spontaneous spheroid formation on the LASCol gel is efficient in increasing disc NP-cell and AF-cell phenotypes compared to thin spreading of cells on the AC gel.

Then, we evaluated gene expression in human disc NP cells on the LASCol gel *in vitro*. Real-time RT–PCR displayed mRNA up-regulation of *TGFB1* (chondrogenesis inducer) [46] on the LASCol gel relative to on the AC gel and non-coated control at 72 h (LASCol versus AC, $P = 0.03$; versus control, $P = 0.009$). In addition, *SOX9* (chondrogenesis regulator) [44], *COMP* (cartilage turnover marker) [45], and *TGFB1* mRNA expression on the LASCol gel was up-regulated relative to on the AC gel and non-coated control at 168 d (*SOX9*: LASCol versus AC, $P = 0.04$; versus control, $P = 0.02$) (*COMP*: LASCol versus AC, $P = 0.02$; versus control, $P = 0.01$) (*TGFB1*: LASCol versus AC, $P = 0.01$; versus control, $P = 0.02$). These gene expression on the LASCol gel all showed time-dependent up-regulation between 72 and 168 h (*SOX9*, $P = 0.001$; *COMP*, $P = 0.003$; *TGFB1*, $P = 0.002$) (Fig. 3D). Spheroid-forming cultures on the LASCol gel stimulate chondrogenic growth of disc NP cells.

3.3. Delayed loss of radiographic disc height and MRI disc intensity by LASCol in a rat tail nucleotomy model

Based on a distinct spheroid-forming and phenotype-preserving characteristics of human disc NP and AF cells on LASCol *in vitro*, an *in-vivo* study was designed using a rat tail nucleotomy model of disc damage which is well established because of the easy accessibility and high reproducibility [37,38]. First, radiographic analysis for the intradiscal 15-μl injection of 21.0-mg/ml LASCol gel, 7.0-mg/ml AC gel, and solvent control after nucleotomy was performed to assess effects of materials. For radiographic disc height measurements using DHI [49] (Fig. 4A), the intra-observer reliability was 0.913–0.947 by intraclass correlation coefficient while the inter-observer reliability was 0.934, all values of which indicated an acceptable reproducibility. Time-course radiographs demonstrated progressive disc space narrowing in solvent control discs (normalized %DHI at 7 d, 65.8 ± 8.0%; 56 d, 50.2 ± 11.9%) but relatively maintained disc height in LASCol-injected (normalized %DHI at 7 d, 78.6 ± 6.7%; 56 d, 77.4 ± 11.4%) and AC-injected discs (normalized %DHI at 7 d, 73.9 ± 9.8%; 56 d, 71.8 ± 11.5%) (Fig. 4BC). These normalized %DHI values were higher in LASCol-injected than control discs at 7–56 d (7 d, $P = 0.005$; 14 d, $P = 0.003$; 28 d, $P = 0.002$; 56 d, $P < 0.001$). Meanwhile, statistical difference in normalized %DHI between AC-injected and control discs was detected only at 56 d ($P = 0.001$) (Fig. 4C). Intradiscal injection of LASCol or AC expedites the maintenance of rat tail disc height.

Next, radiographic analysis for the intradiscal 15-μl injection of LASCol gels at varying 7.0–42.0-mg/ml concentrations after nucleotomy was performed to assess dose-dependent effects of LASCol. Time-course radiographs identified dose-dependent maintenance of height in LASCol-injected discs (normalized %DHI at 56 d in 42.0 mg/ml, 74.4 ± 8.2%; 21.0 mg/ml, 71.9 ± 7.8%; 14.0 mg/ml, 66.0 ± 5.2%; 7.0 mg/ml, 55.7 ± 11.2%) (Fig. 4DE). In fact, normalized %DHI values were higher in 42.0-mg/ml than in 7.0-mg/ml LASCol-injected discs at 7–56 d (7 d, $P = 0.02$; 14 d, $P < 0.001$; 28 d, $P = 0.004$; 56 d, $P = 0.008$). Similarly, statistical difference in normalized %DHI between 21.0-mg/ml and 7.0-mg/ml LASCol-injected discs was observed at 14–56 d (14 d, $P = 0.01$; 28 d, $P = 0.003$; 56 d, $P = 0.02$) (Fig. 4E). Based on these findings, 21.0 mg/ml is proposed as a minimum requirement of intradiscal LASCol concentration.

To find clinically relevant differences between intradiscal LASCol and AC injection, MRIs were taken at 28 d. On T2-weighted images, LASCol-injected discs had higher intensity compared to solvent control discs, indicating preserved disc hydration (Fig. 4F). On T2-mapping images, LASCol-injected discs contained a larger yellow and green area than control discs, indicating a higher water content (Fig. 4F). Then, T2-mapping quantification found statistical T2-value difference between LASCol-injected and control discs ($P = 0.03$), although T2 values in all experimental discs were lower than intact discs (intact [33.7 ± 3.6 ms] versus LASCol [25.7 ± 4.0 ms], $P = 0.001$; versus AC [21.5 ± 1.9 ms], $P < 0.001$; versus control [20.5 ± 1.6 ms], $P < 0.001$) (Fig. 4G). No osteophyte, neoplasm, or abnormal granulation was found in LASCol-injected discs. Radiographic and MRI findings indicate a reduced nucleotomy-induced disc disruption by LASCol, which is equal or better than AC.

3.4. Delayed loss of cell number and safranin-O-positive matrix by LASCol in the disc NP of a rat tail nucleotomy model

We then assessed rat tail LASCol-injected, AC-injected, and solvent control disc histomorphology by safranin-O, fast green, and hematoxylin staining to demonstrate proteoglycan distribution. In LASCol-injected discs, the presence of the LASCol gel was implicated as a safranin-O-negative NP region at 0 and 3 d. In particular, cell migration into the LASCol gel at 3 d was noteworthy (Fig. 5AB). At 7–56 d, safranin-O-positive matrix with cell migration was observed in LASCol-injected discs (Fig. 5AB). In AC-injected discs, the presence of the AC gel was similarly speculated at 0–7 d. However, only a few cells were found on the AC-gel surface at 3 and 7 d (Fig. 5AB). At 14–56 d, AC-injected discs also presented safranin-O-positive matrix; however, the area and cell number were substantially smaller than in LASCol-injected discs (Fig. 5AB). Meanwhile, control discs showed a gross loss, increased clefts, and progressive collapse of NP matrix throughout the study period (Fig. 5AB). Semi-quantification analysis found a reduced loss of cell number in the NP region of LASCol-injected discs compared to AC-injected and control discs at 7–56 d (cell number at 56 d in LASCol, 70.0 ± 15.5; AC, 26.2 ± 9.4; control, 3.2 ± 2.6) (all $P < 0.001$) (Fig. 5C). Delayed loss of safranin-O-positive disc NP area was also observed in LASCol-injected discs relative to AC-injected and control discs at 7–56 d (disc NP area at 56 d in LASCol, 251.6 ± 67.7 × 10^3 μm^2; AC, 72.2 ± 41.5 × 10^3 μm^2; control, 3.8 ± 3.0 × 10^3 μm^2) (all $P < 0.001$) (Fig. 5D). Marked histomorphological differences between LASCol and AC treatments suggest the future potential of LASCol for viable disc tissue repair by the scaffold only.

3.5. Decreased collagen type I-based LASCol and increased collagen type II-positive matrix in the disc NP of a rat tail nucleotomy model

On the basis of histomorphological findings, we performed multicolor immunofluorescence for collagen types I and II to identify injected LASCol and AC gels, which were both developed from collagen type I. In LASCol-injected discs at 0 d, there was the collagen type I-positive, type II-negative structure, indicating the LASCol gel. The gel structure

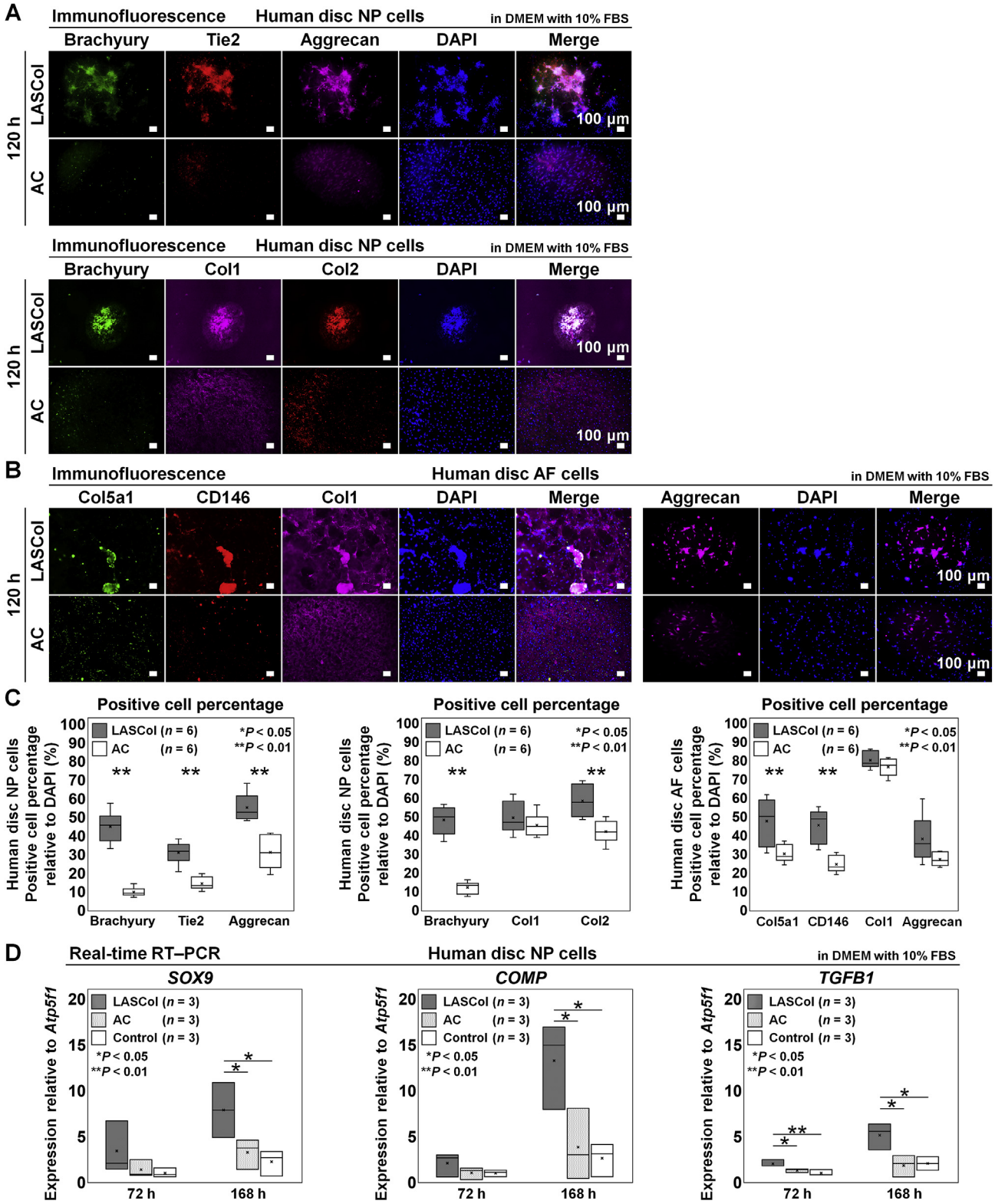

Fig. 3. Enhanced disc-cell and chondrocyte phenotype of human disc NP and AF cells on LASCol. (A) Immunofluorescence of human disc NP cells cultured on the LASCol or AC gel in 10% FBS-supplemented DMEM at 120 h for brachyury (green), Tie2 (red), aggrecan (purple), DAPI (blue), and merged signals and for brachyury (green), collagen type I (purple), collagen type II (red), DAPI (blue), and merged signals. (B) Immunofluorescence of human disc AF cells cultured on the LASCol or AC gel in 10% FBS-supplemented DMEM at 120 h for collagen type V alpha 1 (green), CD146 (red), collagen type I (purple), DAPI, and merged signals and for aggrecan (purple), DAPI, and merged signals. (C) Changes in the percentage of human disc NP cells positive for brachyury, Tie2, aggrecan, and collagen types I and II and AF cells positive for collagen type V alpha 1, CD146, collagen type I, and aggrecan on the LASCol or AC gel. Immunopositivity was counted in five random low-power fields (× 100) and calculated as relative to the total number of DAPI-positive cells. Data are presented with box plots ($n = 6$). The Student t-test was used. (D) Real-time RT–PCR for *SOX9*, *COMP*, and *TGFB1* in total RNA extracts from human disc NP cells cultured on the LASCol or AC gel in 10% FBS-supplemented DMEM at 72 and 168 h. The *ATP5F1* was used as an internal control. Changes in *SOX9/ATP5F1*, *COMP/ATP5F1*, and *TGFB1/ATP5F1* mRNA expression relative to the non-coated control are shown. Data are presented with box plots ($n = 3$). Two-way repeated measures ANOVA with the Tukey–Kramer post-hoc test was used. (For interpretation of the references to color in this figure legend, the reader is referred to the Web version of this article.)

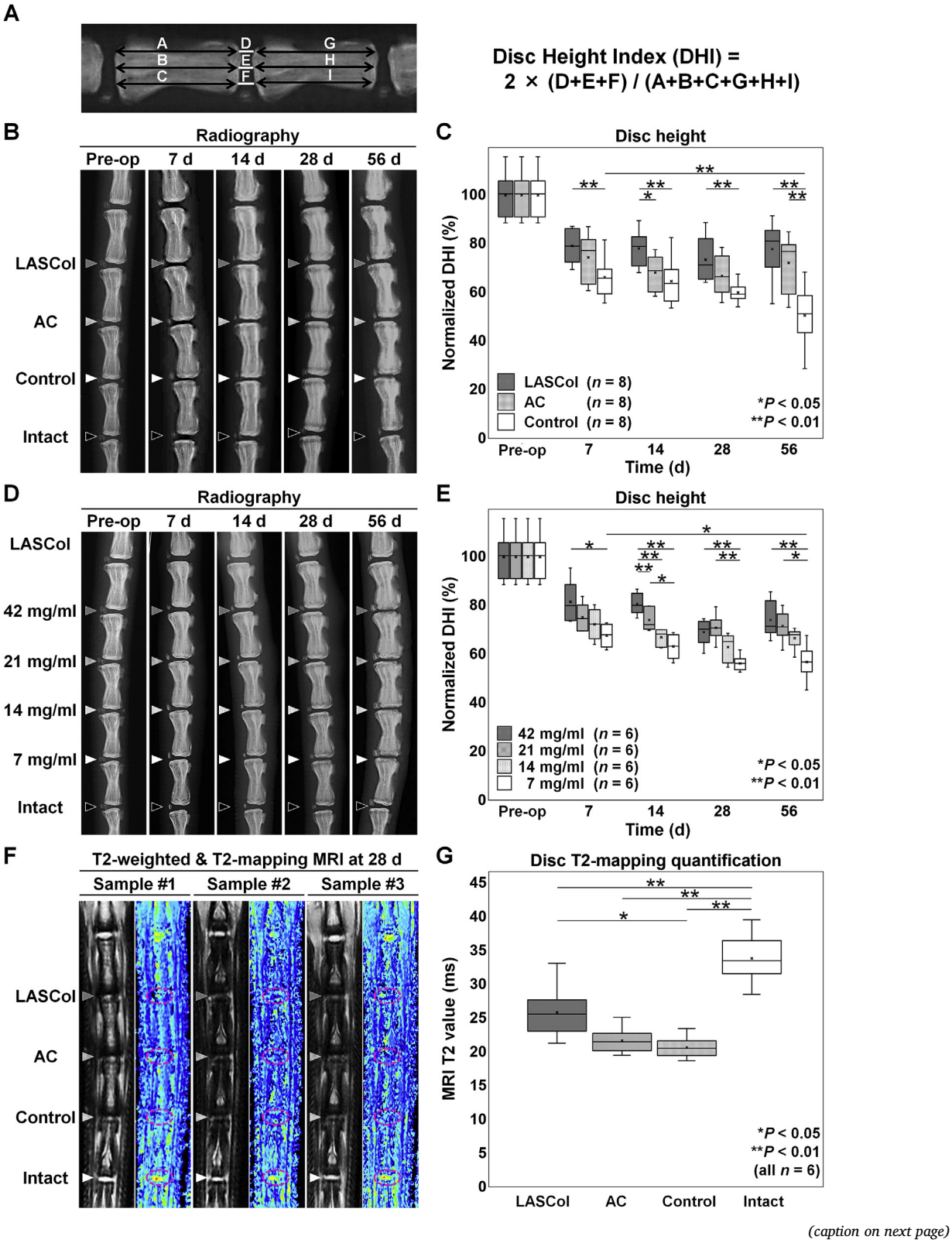

(caption on next page)

underwent progressive DAPI-positive cell migration at 3 d. Then, accelerated disappearance of the collagen type I-positive region and complementary appearance of collagen type II-positive disc NP matrix were observed at 7 d (Fig. 6). In AC-injected discs at 0 d, the collagen type I-positive, type II-negative structure relatively remained unchanged during the initial 7 d, the disappearance of which was decelerated compared to in LASCol-injected discs. There were also no obvious increases in collagen type II expression. Cell migration was found only on the gel-structure surface (Fig. 6). Meanwhile, in control discs, collagen types I and II expression was not clearly detected throughout possibly because of extensive nucleotomy (Fig. 6). Biochemical analysis further clarifies the future potential of collagen type I-positive LASCol for biological tissue repair with collagen type II-positive NP-like tissues.

Fig. 4. Delayed loss of radiographic disc height and MRI disc intensity by LASCol in a rat tail nucleotomy model. (A) The disc height index (DHI) was calculated by measuring, averaging, and normalizing the disc heights to the adjacent vertebral body heights at the anterior, middle, and posterior portions. (B) Lateral radiographs of rat tail 15-μl LASCol-injected (21.0 mg/ml), AC-injected (7.0 mg/ml), and solvent control discs taken before (pre-operation [pre-op]) and at 7, 14, 28, or 56 d after nucleotomy. Dark-gray, light-gray, white, and black triangles indicate LASCol-injected, AC-injected, solvent control, and untreated intact discs, respectively. (C) Changes in %DHI of LASCol-injected, AC-injected, and control discs. (D) Lateral radiographs of rat tail 15-μl LASCol-injected discs at varying concentrations (42.0, 21.0, 14.0, and 7.0 mg/ml) taken before (pre-operation [pre-op]) and at 7, 14, 28, or 56 d after nucleotomy. Dark-gray, intermediate-gray, light-gray, white, and black triangles indicate 42.0-mg/ml, 21.0-mg/ml, 14.0-mg/ml, and 7.0-mg/ml LASCol-injected, and untreated intact discs, respectively. (E) Changes in %DHI of LASCol-injected discs at varying concentrations. (F) Sagittal T2-weighted and T2-mapping MRIs of rat tail 15-μl LASCol-injected (21.0 mg/ml), AC-injected (7.0 mg/ml), and solvent control discs taken at 28 d after nucleotomy. Dark-gray, intermediate-gray, light-gray, and white triangles indicate LASCol-injected, AC-injected, solvent control, and untreated intact discs, respectively. Pink circles indicate the respective discs in T2-mapping images. (G) Changes in T2-mapping value of LASCol-injected, AC-injected, control, and intact discs. In (C), (E), and (G), data are presented with box plots (c, $n = 8$; e, $n = 6$; g, $n = 6$). Two-way repeated measures ANOVA with the Tukey–Kramer post-hoc test was used for (C) and (E). One-way ANOVA with the Tukey–Kramer post-hoc test was used for (G). (For interpretation of the references to color in this figure legend, the reader is referred to the Web version of this article.)

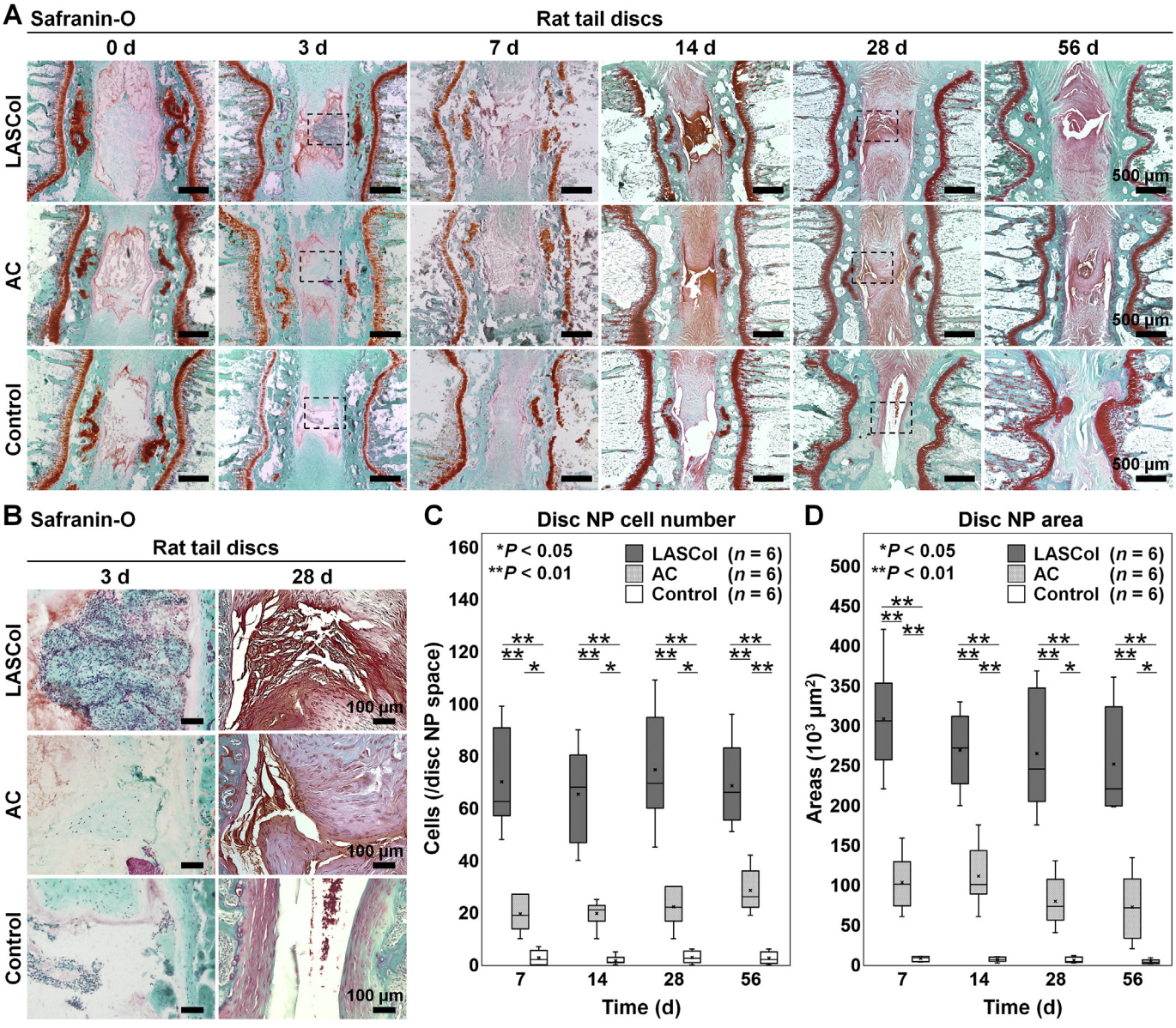

Fig. 5. Delayed loss of cell number and Safranin-O-positive matrix by LASCol in the disc NP of a rat tail nucleotomy model. (A) Safranin-O staining of rat tail 15-μl LASCol-injected (21.0 mg/ml), AC-injected (7.0 mg/ml), and solvent control discs sectioned at 0, 3, 7, 14, 28, or 56 d after nucleotomy in low-power fields (× 100). Black rectangles indicate the disc NP area shown as high-power field images in Fig. 5B. (B) Safranin-O staining of rat tail 15-μl LASCol-injected, AC-injected, and solvent control discs sectioned at 3 and 28 d after nucleotomy in high-power fields (× 400). (C) Changes in the number of cells in LASCol-injected, AC-injected, and control disc NP spaces. (D) Changes in safranin-O-positive area of LASCol-injected, AC-injected, and control disc NP spaces. In (C) and (D), data are presented with box plots ($n = 6$). Two-way repeated measures ANOVA with the Tukey–Kramer post-hoc test was used.

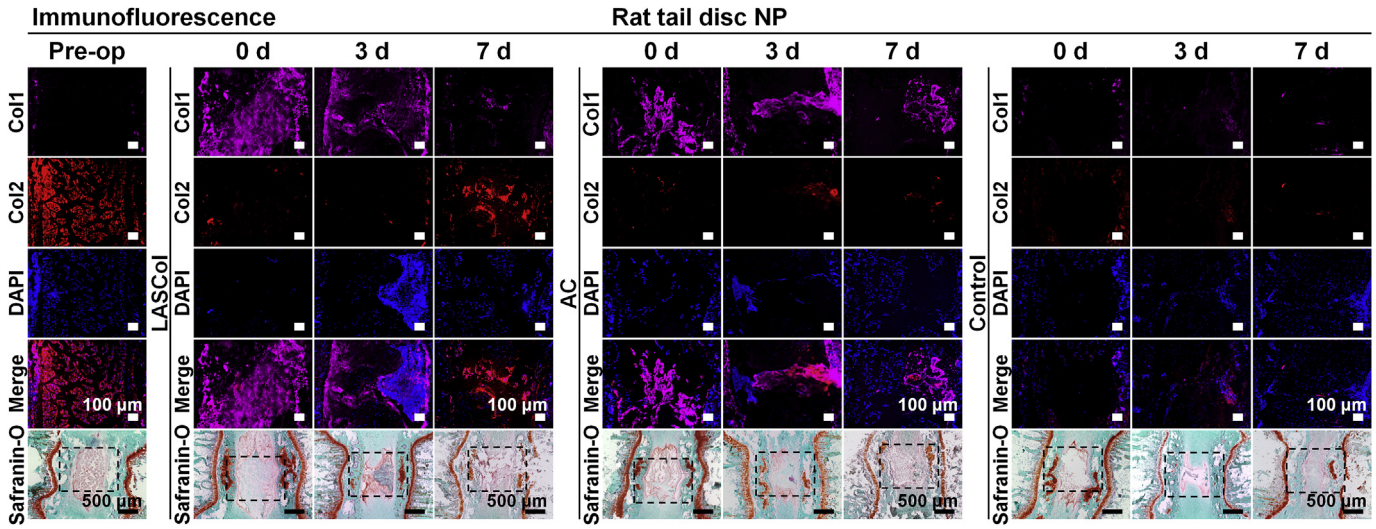

Fig. 6. Decreased collagen type I-based LASCol and increased collagen type II-positive matrix in the disc NP of a rat tail nucleotomy model. Immunofluorescence of rat tail 15-μl LASCol-injected (21.0 mg/ml), AC-injected (7.0 mg/ml), and solvent control discs sectioned before (pre-operation [pre-op]) and at 0, 3, or 7 d after nucleotomy for collagen type I (purple), collagen type II (red), DAPI (blue), and merged signals. The LASCol and AC consist of collagen type I. Black rectangles indicate the disc NP area analyzed by immunofluorescence. (For interpretation of the references to color in this figure legend, the reader is referred to the Web version of this article.)

3.6. Migration of cells with the endogenous phenotype into LASCol in the disc NP of a rat tail nucleotomy model

Next, we performed multi-color immunofluorescence for brachyury, Tie2, and aggrecan to assess the phenotype of migrated cells into the LASCol gel. First, we thought these cells as remnant disc NP cells. In LASCol-injected discs, a substantial percentage of cells were brachyury-positive (3 d, 36.4 ± 9.9%; 7 d, 37.1 ± 4.8%; 14 d, 34.0 ± 8.3%; 28 d, 32.0 ± 4.5%; 56 d, 27.9 ± 5.2%), Tie2-positive (3 d, 39.7 ± 5.5%; 7 d, 22.7 ± 7.0%; 14 d, 20.3 ± 3.2%; 28 d, 22.2 ± 4.3%; 56 d, 17.7 ± 3.2%), and aggrecan-positive (3 d, 48.2 ± 6.2%; 7 d, 42.0 ± 5.4%; 14 d, 41.7 ± 8.6%; 28 d, 39.5 ± 4.6%; 56 d, 36.8 ± 3.2%) (Fig. 7AB). However, in AC-injected discs, immunopositivity for brachyury (3 d, 18.9 ± 3.7%; 7 d, 15.9 ± 3.1%; 14 d, 13.7 ± 3.7%; 28 d, 13.1 ± 2.3%; 56 d, 11.6 ± 1.6%), Tie2 (3 d, 15.0 ± 5.6%; 7 d, 10.1 ± 3.8%; 14 d, 11.9 ± 2.5%; 28 d, 7.5 ± 1.6%; 56 d, 6.1 ± 3.1%), and aggrecan (3 d, 29.9 ± 8.6%; 7 d, 31.3 ± 6.0%; 14 d, 29.6 ± 3.9%; 28 d, 28.3 ± 4.8%; 56 d, 26.0 ± 5.6%) was statistically lower than in LASCol-injected discs (all $P < 0.01$) (Fig. 7AB). Similarly, in control discs, immunopositivity for brachyury (3 d, 8.9 ± 2.4%; 7 d, 13.8 ± 4.8%; 14 d, 11.4 ± 3.2%; 28 d, 9.9 ± 2.0%; 56 d, 8.5 ± 2.0%), Tie2 (3 d, 8.4 ± 3.7%; 7 d, 11.7 ± 3.5%; 14 d, 8.5 ± 1.2%; 28 d, 5.5 ± 2.5%; 56 d, 7.0 ± 2.7%), and aggrecan (3 d, 16.3 ± 3.0%; 7 d, 16.2 ± 5.3%; 14 d, 17.2 ± 5.6%; 28 d, 14.0 ± 3.5%; 56 d, 9.1 ± 4.1%) was further low compared to in LASCol-injected discs (all $P < 0.001$) (Fig. 7AB). The presence of cells with brachyury-positive and/or Tie2-positive disc NP phenotypes supports the accelerated migration of remnant cells through LASCol-mediated spontaneous spheroid formation, potentially contributing to the repair process of nucleotomy-induced disc damage by expressing aggrecan as well as collagen type II.

3.7. Infiltration of macrophages into LASCol in the disc NP of a rat tail nucleotomy model

We further performed additional multi-color immunofluorescence for macrophage markers to identify residual cell migration other than remnant disc NP cells. In LASCol-injected discs, Iba1 (pan-macrophage marker) [41] was positive in a substantial percentage of cells into the LASCol gel (3 d, 59.6 ± 3.8%; 7 d, 67.9 ± 6.7%; 14 d, 58.7 ± 6.9%; 28 d, 48.0 ± 8.5%; 56 d, 32.2 ± 6.0%). This immunopositivity for Iba1 increased from 3 to 7 d ($P = 0.04$), indicating progressive macrophage infiltration to possibly accelerate LASCol degradation at earlier time points and gradual reduction of macrophages from 14 to 56 d after surgery. Moreover, cells in part were positive for CD86 (M1-polarized macrophage marker for pro-inflammation) [42] (3 d, 34.3 ± 6.0%; 7 d, 35.1 ± 5.3%; 14 d, 31.1 ± 4.5%; 28 d, 23.9 ± 3.3%; 56 d, 16.8 ± 4.2%) and/or CD163 (M2-polarized macrophage marker for anti-inflammation and tissue remodeling) [43] (3 d, 26.3 ± 4.5%; 7 d, 24.2 ± 5.5%; 14 d, 28.6 ± 5.0%; 28 d, 21.7 ± 4.6%; 56 d, 17.5 ± 4.0%) (Fig. 8AB). In AC-injected discs, cells observed on the gel surface were also Iba1-positive (3 d, 33.9 ± 7.0%; 7 d, 27.9 ± 10.8%; 14 d, 28.7 ± 6.3%; 28 d, 29.3 ± 5.7%; 56 d, 18.5 ± 4.2%), although the percentage was lower than in LASCol-injected discs (all $P < 0.001$). Immunopositivity for CD86 (3 d, 20.0 ± 3.1%; 7 d, 17.7 ± 7.9%; 14 d, 18.9 ± 3.6%; 28 d, 19.0 ± 4.9%; 56 d, 12.5 ± 3.5%) and CD163 (3 d, 14.9 ± 2.9%; 7 d, 9.9 ± 3.5%; 14 d, 9.7 ± 3.4%; 28 d, 14.0 ± 3.1%; 56 d, 8.0 ± 3.0%) was further low (CD86: 3–14 d, $P < 0.001$; 28 d, $P = 0.046$; 56 d, $P = 0.08$; CD163: all $P < 0.001$) (Fig. 8AB). There were few Iba1-positive cells in control discs (3 d, 20.1 ± 5.5%; 7 d, 24.1 ± 7.0%; 14 d, 12.8 ± 4.9%; 28 d, 15.6 ± 5.0%; 56 d, 12.1 ± 3.8%) compared to in LASCol-injected discs (all $P < 0.001$). Immunopositivity for CD86 (3 d, 10.5 ± 3.8%; 7 d, 11.8 ± 4.0%; 14 d, 7.7 ± 3.5%; 28 d, 9.7 ± 3.5%; 56 d, 8.8 ± 4.3%) and CD163 (3 d, 9.0 ± 3.6%; 7 d, 8.2 ± 1.9%; 14 d, 4.4 ± 3.0%; 28 d, 6.3 ± 3.3%; 56 d, 6.7 ± 2.4%) was also lower (all $P < 0.001$) (Fig. 8AB). In our proposed model, LASCol-mediated infiltration of M1-polarized and also M2-polarized macrophages would serve for the LASCol self-biodegradation. This could also be beneficial for the tissue repair process, in particular by M2-polarized macrophages. However, effectiveness of macrophage infiltration-mediated secondary inflammatory responses for the disc requires careful evaluations in the future.

4. Discussion

This is the first study to demonstrate the potential for intervertebral disc damage control by LASCol. In *in-vitro* experiments, compared to

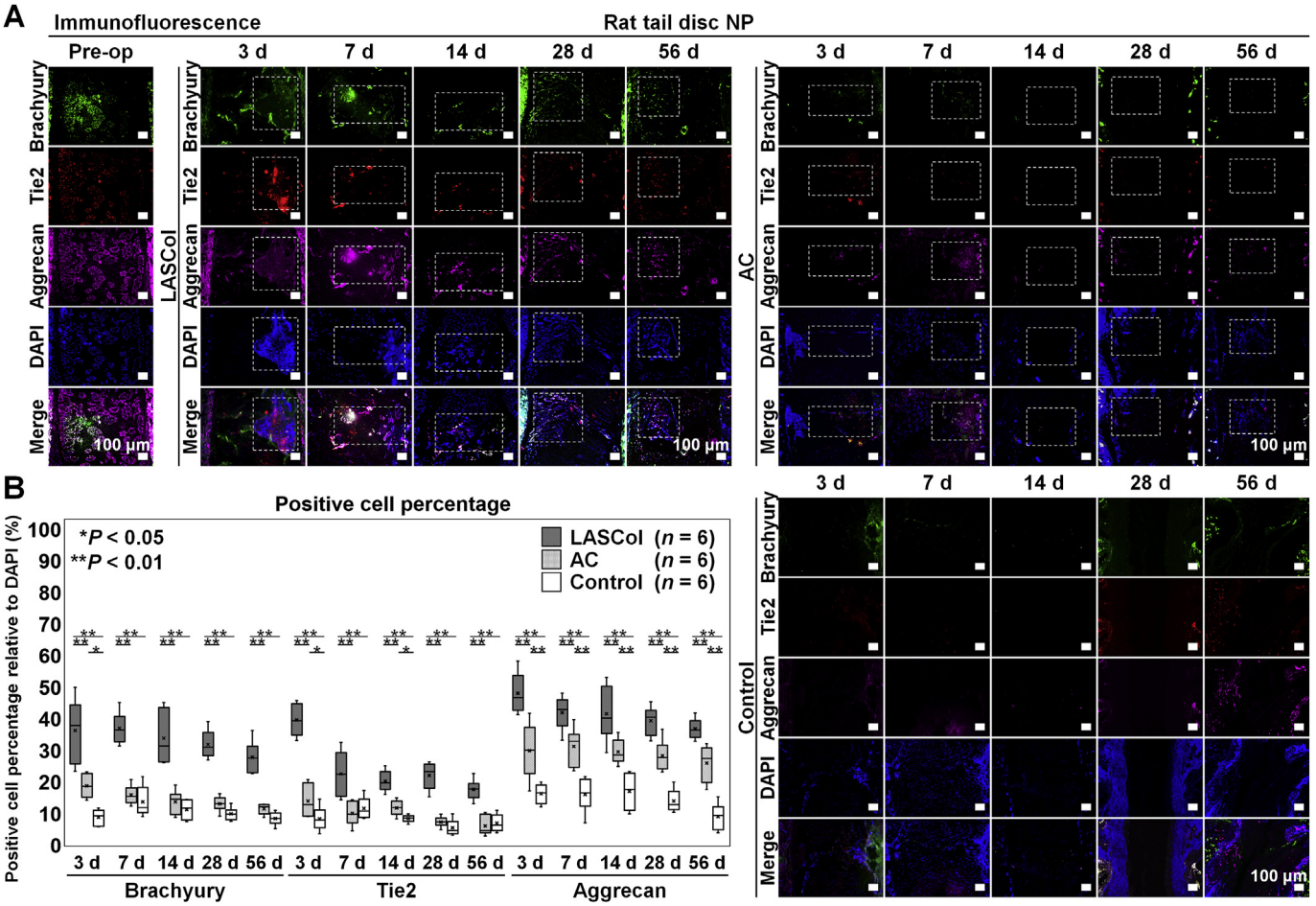

Fig. 7. Migration of cells with the endogenous phenotype into LASCol in the disc NP of a rat tail nucleotomy model. (A) Immunofluorescence of rat tail 15-μl LASCol-injected (21.0 mg/ml), AC-injected (7.0 mg/ml), and solvent control discs sectioned before (pre-operation [pre-op]) and at 3, 7, 14, 28, or 56 d after nucleotomy for brachyury (green), Tie2 (red), aggrecan (purple), DAPI (blue), and merged signals. White rectangles indicate the LASCol or AC gel. (B) Changes in the percentage of cells in LASCol-injected, AC-injected, and control disc NP spaces positive for brachyury, Tie2, and aggrecan. Immunopositivity was counted in the whole disc NP low-power fields (× 100) and calculated as relative to the total number of DAPI-positive cells. Data are presented with box plots ($n = 6$). Two-way repeated measures ANOVA with the Tukey–Kramer post-hoc test was used. (For interpretation of the references to color in this figure legend, the reader is referred to the Web version of this article.)

AC, LASCol induced the formation of spheroids with an increased expression of human disc NP-cell and AF-cell phenotypes. In this study, the ratio of Tie2-positive cells on the LASCol gel was higher than that in other reports [9]. As Tie2 expresses at early phases of nucleus pulposus differentiation, LASCol-mediated spheroid formation appears to stimulate the progenitor potential, requiring further mechanistic investigations. In *in-vivo* experiments, LASCol induced a delayed progression of disc damage in a rat tail nucleotomy model. Radiographic and MRI findings were relatively similar between LASCol and AC, indicating the difficulty of complete structural disc repair by the applied version (concentration, dose, and volume) of both materials—a subject to be studied in the future. However, LASCol had distinct histological differences from AC in the cell number and matrix area of the disc NP. Furthermore, time-course histomorphology and immunofluorescence disclosed a marked migration of endogenous disc NP cells expressing aggrecan and collagen type II and infiltration of M1-polarized and also M2-polarized macrophages into LASCol with an accelerated degradation of collagen type I-positive LASCol. The observed reduction in structural disc damage and spontaneous invasion of endogenous cells and macrophages including the M2 by LASCol, suggesting the future potential for viable disc repair, is notable based on the spheroid-forming capability [22]. A stem cell-seeded tissue-engineered scaffold reports the maintenance of mechanical function and integration up to eight weeks [52]. Hyaluronan-based [53] and alginate-based [54] scaffolds present with enhanced NP-cell phenotypes and matrix production. These scaffolds with a disc regenerative potential are attractive; however, their repair mechanisms have not been fully clarified. At least, no scaffolds other than LASCol have shown spontaneous spheroid formation. While recent advances in the application of stem cells and/or growth factors have enabled radiographic disc height and MRI signal restoration, disc-specific phenotype maintenance, and increased matrix expression in animals [21] and discogenic pain relief and MRI signal improvement in humans [20], these treatments require the specialized institutions, equipment, scientists, technicians, strict laws and regulations, numerous medical expenses, and nevertheless unfavorable health complications. However, LASCol could stimulate disc-cell migration and disc-tissue repair by the scaffold only through a simple, temperature-sensitive gel injection. In addition, treatment of LASCol, developed from abundantly available porcine skin's collagen type I, is much less expensive than cell transplantation and/or growth factor administration. Therefore, intradiscal LASCol injection is a new scaffold treatment option for non-critical but highly prevalent, intervertebral disc disease.

In this study, *in-vivo* delayed reduction of safranin-O-positive matrix by LASCol is speculated to come from cells migrating into LASCol expressing aggrecan and collagen type II as well as brachyury and/or Tie2, similar to endogenous disc NP cells. The LASCol would promote the internal migration of remnant disc NP cells, accelerate the formation of cell-aggregating spheroids encouraging the original disc NP

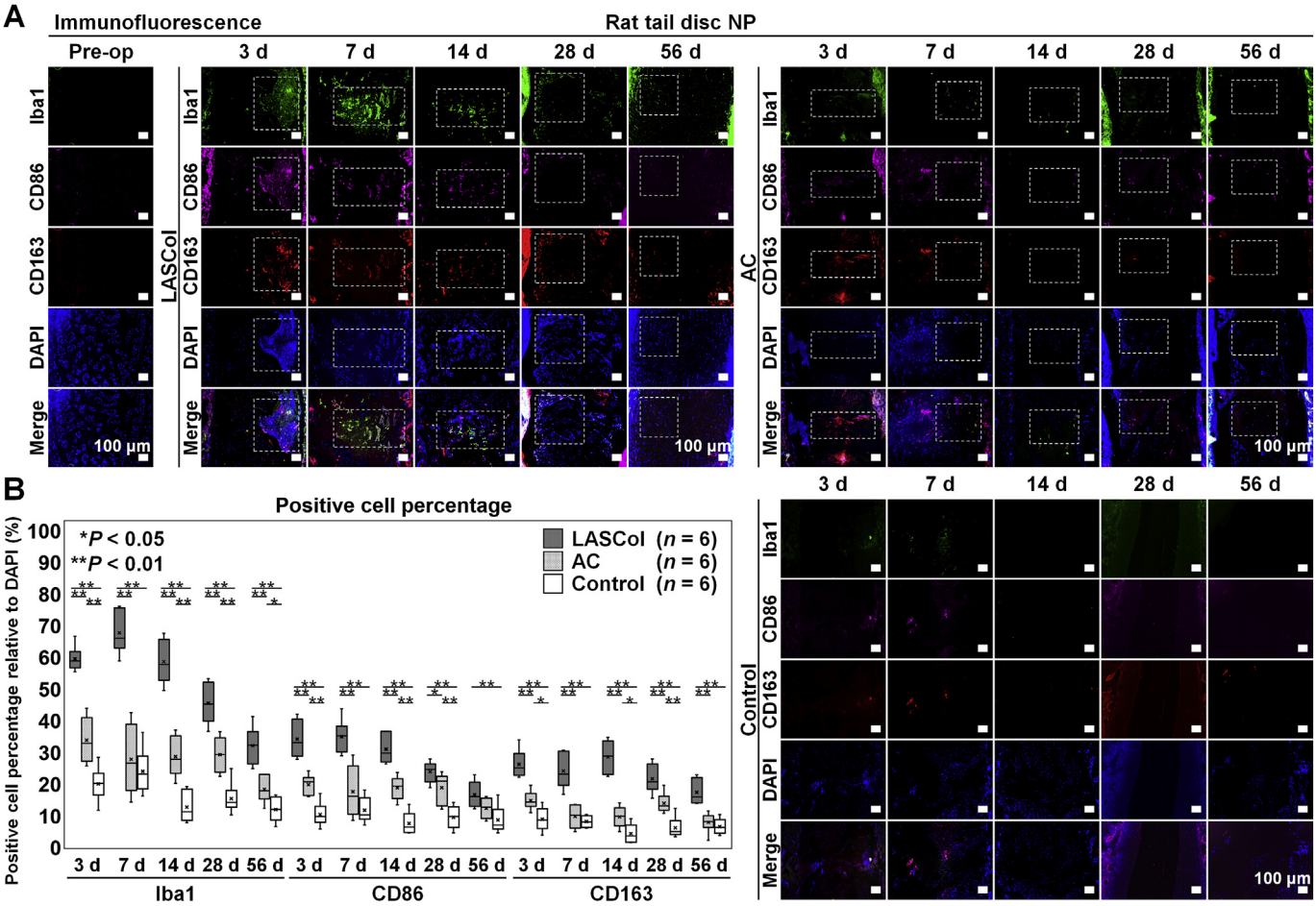

Fig. 8. Infiltration of macrophages into LASCol in the disc NP of a rat tail nucleotomy model. (A) Immunofluorescence of rat tail 15-μl LASCol-injected (21.0 mg/ml), AC-injected (7.0 mg/ml), and solvent control discs sectioned before (pre-operation [pre-op]) and at 3, 7, 14, 28, or 56 d after nucleotomy for Iba1 (green), CD86 (purple), CD163 (red), DAPI (blue), and merged signals. White rectangles indicate the LASCol or AC gel. (B) Changes in the percentage of cells in LASCol-injected, AC-injected, and control disc NP spaces positive for Iba1, CD86, and CD163. Immunopositivity was counted in the whole disc NP low-power fields (× 100) and calculated as relative to the total number of DAPI-positive cells. Data are presented with box plots (n = 6). Two-way repeated measures ANOVA with the Tukey–Kramer post-hoc test was used. (For interpretation of the references to color in this figure legend, the reader is referred to the Web version of this article.)

phenotype maintenance, e.g. brachyury$^+$, Tie2$^+$, aggrecan$^+$, and collagen type II$^+$, and also up-regulating chondrogenic *SOX9*, *COMP*, and *TGFB1* gene expression, and facilitate viable disc-tissue repair with the presence of matrix-producing cells. Consequently, this treatment is potentially suitable for discs with early to intermediate stages of degeneration that cells can still be alive [55]. Long-term effectiveness of LASCol to prevent the progression of age-dependent disc degeneration should be studied in the future.

When the efficacy of LASCol depends on endogenous disc NP-cell migration and aggrecan-positive and collagen type II-positive tissue repair, rapid self-biodegradation of collagen type I-based LASCol is advantageous to restore the original tissue environment as the difference in biochemical characteristics between collagen types I (two pro-alpha 1[I] chains and one pro-alpha 2[I] chain) and II (homotrimers of alpha 1[II] chains) is distinct [56]. In this study, infiltration of M2-polarized macrophages as well as M1-polarized macrophages into LASCol is a possible approach to accelerate this degradation. As no macrophages exist in healthy discs but marked macrophage infiltration is observed in aged discs, the M1/M2-polarization of macrophages corresponds to the degeneration severity [57]. Of course, macrophage infiltration into the disc induces mechanical hyperalgesia and pro-inflammatory cytokine production [58]. The originally avascular nature of the disc without macrophage infiltration [57,58] requests a careful interpretation on the involvement of secondary inflammatory responses. Nevertheless, the transition of macrophage polarization from a pro-inflammatory M1 to a pro-healing M2 can be a strategy to improve a poor healing potential of the intervertebral disc [57]. In addition, the design of scaffolds is also critical as macrophages acquire a more tissue-regenerative M2-polarized phenotype on scaffolds with larger fiber and pore dimensions [59]. Following further justifications of the 3D microstructure of scaffolds and roles of inflammation in the disc, the infiltration of M1-polarized and also M2-polarized macrophages could prove useful for not only the biodegradation of LASCol but also the repair process of disc tissues.

This study has several limitations. *In vitro*, human disc cells surgically obtained had variations in age, sex, and disc degeneration severity, although the observed findings were consistent regardless of these parameters. *In vivo*, rat tail discs are biologically and mechanically different from rat lumbar discs as well as humans. Rodents retain notochordal cells in the disc NP throughout their lives, resulting in fewer age-related disc pathologies [60]. Mechanical differences between cervical/lumbar and caudal segments and between bipeds and quadrupeds are not negligible [60]. In addition, surgical induction of nucleotomy-induced disc disruption in rat tails does not completely mimic clinical situation of degenerative and herniated discs in humans [61]. Therefore, preclinical studies of LASCol using larger-sized animal models in which disc NP notochordal cells disappear should be carried out. In this study, despite the observed *in-vitro* compatibility of LASCol with both disc NP and AF cells, *in-vivo* analysis was primarily focused on disc NP tissues, requiring future clarifications regarding LASCol-

mediated disc repair. Further biomechanical and structural analyses of intradiscal LASCol also need to be conducted. As the material property, alternative LASCol based on collagen type II but not type I might be preferable to repair disc NP tissues since disc NP matrix comprises collagen type II. The development of collagen type II-based LASCol is technically capable; however, the quality control and mass production are difficult due to a limited acquisition amount of raw materials, e.g. pig knee articular cartilage. Collagen type I-based LASCol can be supplied stably and affordably for future clinical applications. It should also be determined in the future which is the best suited shape to the future clinical intradiscal application of LASCol, injectable gel or other shapes including sponge, fragment, flake, and powder.

5. Conclusion

The LASCol, a new collagen type I-based scaffold that we developed by actinidain hydrolysis, has distinct characteristics from conventional AC of an improved water-solubility, faster biodegradability, decreased antigenicity, and then marked capability of 3D spheroid formation by the scaffold only. This first, preliminary study of LASCol-mediated intervertebral disc repair demonstrated spontaneous spheroid formation and enhanced phenotypic characteristics of human intervertebral disc NP and AF cells surgically collected. In a rat tail model of disc disruption by nucleotomy, LASCol-injected discs presented with a reduced radiological and histological damage, showing the migration into LASCol of aggrecan-positive and collagen type II-positive endogenous disc NP cells, as well as an accelerated biodegradation of LASCol with the infiltration of M1-polarized and also M2-polarized macrophages. Following future mechanistic studies using larger-sized animal models and finally human trials, simple intradiscal injection of LASCol may be an effective treatment option without any transplantation of stem cells and/or administration of growth factors for intervertebral disc disease.

Author contributions

Y.T., T.Y., K.M., S.K., M.F., and R.K. designed the study; Y.T. and T.Y. performed the *in-vitro* and *in-vivo* experiments; K.M. and S.K. performed the material development; Y.T., T.Y., K.M., S.K., Y.Kanda, R.T., Y.K., N.F., T.T., K.O., Y.Kakiuchi, S.M., K.K., T.T., K.N., M.F., and R.K. contributed to the data analysis and interpretation; and Y.T. and T.Y. wrote the manuscript.

Competing financial interests

The authors declare no competing financial interests.

Data availability

The raw/processed data required to reproduce these findings cannot be shared at this time as the data also forms part of an ongoing study.

Acknowledgements

The authors thank Dr. Yohei Kumabe and Mses. Kyoko Tanaka, Maya Yasuda, and Minako Nagata (Department of Orthopaedic Surgery, Kobe University Graduate School of Medicine, Kobe, Japan) for their technical assistance and Messrs. Akira Hirakimoto and Jiro Wada (Kobe University, Kobe, Japan), Messrs. Masaki Hirokoh and Hiroyuki Ito (Kindai University, Higashi-Osaka, Japan), and Mr. Atsuo Yamanaka (TRI, Kobe, Japan) for their intellectual property strategy support. This work was supported by JSPS KAKENHI Grant Number JP18K16659 (T.Y.) and Adaptable and Seamless Technology Transfer Program through Target-driven R&D from Japan Science and Technology Agency Grant Numbers AS2414037P and AS2715177U (K.M.).

Appendix A. Supplementary data

Supplementary data to this article can be found online at https://doi.org/10.1016/j.biomaterials.2020.119781.

References

[1] G.B. Andersson, Epidemiological features of chronic low-back pain, Lancet 354 (9178) (1999) 581–585.
[2] J.N. Katz, Lumbar disc disorders and low-back pain: socioeconomic factors and consequences, J. Bone Joint Surg. Am. 88 (Suppl 2) (2006) 21–24 Suppl 2.
[3] G. Livshits, M. Popham, I. Malkin, P.N. Sambrook, A.J. Macgregor, T. Spector, F.M. Williams, Lumbar disc degeneration and genetic factors are the main risk factors for low back pain in women: the UK Twin Spine Study, Ann. Rheum. Dis. 70 (10) (2011) 1740–1745.
[4] J.A. Saal, J.S. Saal, Nonoperative treatment of herniated lumbar intervertebral disc with radiculopathy. An outcome study, Spine (Phila Pa 1976 14 (4) (1989) 431–437.
[5] J.P. Urban, S. Roberts, Degeneration of the intervertebral disc, Arthritis Res. Ther. 5 (3) (2003) 120–130.
[6] C.J. Hunter, J.R. Matyas, N.A. Duncan, Cytomorphology of notochordal and chondrocytic cells from the nucleus pulposus: a species comparison, J. Anat. 205 (5) (2004) 357–362.
[7] K.S. Choi, B.D. Harfe, Hedgehog signaling is required for formation of the notochord sheath and patterning of nuclei pulposi within the intervertebral discs, Proc. Natl. Acad. Sci. U.S.A. 108 (23) (2011) 9484–9489.
[8] M.V. Risbud, Z.R. Schoepflin, F. Mwale, R.A. Kandel, S. Grad, J.C. Iatridis, D. Sakai, J.A. Hoyland, Defining the phenotype of young healthy nucleus pulposus cells: recommendations of the Spine Research Interest Group at the 2014 annual ORS meeting, J. Orthop. Res. 33 (3) (2015) 283–293.
[9] D. Sakai, Y. Nakamura, T. Nakai, T. Mishima, S. Kato, S. Grad, M. Alini, M.V. Risbud, D. Chan, K.S. Cheah, K. Yamamura, K. Masuda, H. Okano, K. Ando, J. Mochida, Exhaustion of nucleus pulposus progenitor cells with ageing and degeneration of the intervertebral disc, Nat. Commun. 3 (1264) (2012) 1264.
[10] G.G. van den Akker, D.A. Surtel, A. Cremers, S.M. Richardson, J.A. Hoyland, L.W. van Rhijn, J.W. Voncken, T.J. Welting, Novel immortal cell lines support cellular heterogeneity in the human annulus fibrosus, PLoS One 11 (1) (2016) e0144497.
[11] T. Nakai, D. Sakai, Y. Nakamura, T. Nukaga, S. Grad, Z. Li, M. Alini, D. Chan, K. Masuda, K. Ando, J. Mochida, M. Watanabe, CD146 defines commitment of cultured annulus fibrosus cells to express a contractile phenotype, J. Orthop. Res. 34 (8) (2016) 1361–1372.
[12] S. Poiraudeau, I. Monteiro, P. Anract, O. Blanchard, M. Revel, M.T. Corvol, Phenotypic characteristics of rabbit intervertebral disc cells. Comparison with cartilage cells from the same animals, Spine 24 (9) (1999) 837–844.
[13] J.P. Urban, S. Smith, J.C. Fairbank, Nutrition of the intervertebral disc, Spine 29 (23) (2004) 2700–2709.
[14] T. Yurube, W.J. Buchser, H.J. Moon, R.A. Hartman, K. Takayama, Y. Kawakami, K. Nishida, M. Kurosaka, N.V. Vo, J.D. Kang, M.T. Lotze, G.A. Sowa, Serum and nutrient deprivation increase autophagic flux in intervertebral disc annulus fibrosus cells: an in vitro experimental study, Eur. Spine J. 28 (5) (2019) 993–1004.
[15] N. Boos, S. Weissbach, H. Rohrbach, C. Weiler, K.F. Spratt, A.G. Nerlich, Classification of age-related changes in lumbar intervertebral discs: 2002 Volvo Award in basic science, Spine 27 (23) (2002) 2631–2644.
[16] K.M. Cheung, J. Karppinen, D. Chan, D.W. Ho, Y.Q. Song, P. Sham, K.S. Cheah, J.C. Leong, K.D. Luk, Prevalence and pattern of lumbar magnetic resonance imaging changes in a population study of one thousand forty-three individuals, Spine 34 (9) (2009) 934–940.
[17] B.P. Bechara, V. Agarwal, J. Boardman, S. Perera, D.K. Weiner, N. Vo, J. Kang, G.A. Sowa, Correlation of pain with objective quantification of magnetic resonance images in older adults with chronic low back pain, Spine 39 (6) (2014) 469–475.
[18] R.A. Deyo, S.K. Mirza, Herniated lumbar intervertebral disk, N. Engl. J. Med. 374 (18) (2016) 1763–1772.
[19] G. Ghiselli, J.C. Wang, N.N. Bhatia, W.K. Hsu, E.G. Dawson, Adjacent segment degeneration in the lumbar spine, J. Bone Joint Surg. Am. 86 (7) (2004) 1497–1503.
[20] D. Sakai, G.B. Andersson, Stem cell therapy for intervertebral disc regeneration: obstacles and solutions, Nat. Rev. Rheumatol. 11 (4) (2015) 243–256.
[21] K. Masuda, Biological repair of the degenerated intervertebral disc by the injection of growth factors, Eur. Spine J. 17 (Suppl 4) (2008) 441–451.
[22] R.D. Bowles, L.A. Setton, Biomaterials for intervertebral disc regeneration and repair, Biomaterials 129 (2017) 54–67.
[23] G. Vadala, G. Sowa, M. Hubert, L.G. Gilbertson, V. Denaro, J.D. Kang, Mesenchymal stem cells injection in degenerated intervertebral disc: cell leakage may induce osteophyte formation, J. Tissue Eng. Regenerat. Med. 6 (5) (2012) 348–355.
[24] C.A. Herberts, M.S. Kwa, H.P. Hermsen, Risk factors in the development of stem cell therapy, J. Transl. Med. 9 (2011) 29.
[25] B. Skovrlj, S.M. Koehler, P.A. Anderson, S.A. Qureshi, A.C. Hecht, J.C. Iatridis, S.K. Cho, Association between BMP-2 and carcinogenicity, Spine (Phila Pa 1976 40 (23) (2015) 1862–1871.
[26] P. Priyadarshani, Y. Li, L. Yao, Advances in biological therapy for nucleus pulposus regeneration, Osteoarthr. Cartil. 24 (2) (2016) 206–212.
[27] Y. Kato, J. Chavez, S. Yamada, S. Hattori, S. Takazawa, H. Ohuchi, A large knee osteochondral lesion treated using a combination of osteochondral autograft

transfer and second-generation autologous chondrocyte implantation: a case report, Regen Ther 10 (2019) 10–16.
[28] Y. Sugata, S. Sotome, M. Yuasa, M. Hirano, K. Shinomiya, A. Okawa, Effects of the systemic administration of alendronate on bone formation in a porous hydroxyapatite/collagen composite and resorption by osteoclasts in a bone defect model in rabbits, J. Bone Joint Surg. Br. 93 (4) (2011) 510–516.
[29] E. Knight, S. Przyborski, Advances in 3D cell culture technologies enabling tissue-like structures to be created in vitro, J. Anat. 227 (6) (2015) 746–756.
[30] S. Kunii, K. Morimoto, K. Nagai, T. Saito, K. Sato, B. Tonomura, Actinidain-hydrolyzed type I collagen reveals a crucial amino acid sequence in fibril formation, J. Biol. Chem. 285 (23) (2010) 17465–17470.
[31] K. Morimoto, S. Kunii, E. Yamamoto, H. Ito, Y. Kuboki, Composition for Inducing Differentiation, US Patent (2018) 10155804.
[32] K. Morimoto, S. Kunii, Latent nature of collagen in promoting three-dimensional adherent spheroid formation of fibroblasts, Materialia 8 (2019) 100450.
[33] J.L. Bron, G.H. Koenderink, V. Everts, T.H. Smit, Rheological characterization of the nucleus pulposus and dense collagen scaffolds intended for functional replacement, J. Orthop. Res. 27 (5) (2009) 620–626.
[34] C.W.A. Pfirrmann, A. Metzdorf, M. Zanetti, J. Hodler, N. Boos, Magnetic resonance classification of lumbar intervertebral disc degeneration, Spine 26 (17) (2001) 1873–1878.
[35] M. Ito, T. Yurube, K. Kakutani, K. Maeno, T. Takada, Y. Terashima, Y. Kakiuchi, Y. Takeoka, S. Miyazaki, R. Kuroda, K. Nishida, Selective interference of mTORC1/RAPTOR protects against human disc cellular apoptosis, senescence, and extracellular matrix catabolism with Akt and autophagy induction, Osteoarthr. Cartil. 25 (12) (2017) 2134–2146.
[36] Y. Kakiuchi, T. Yurube, K. Kakutani, T. Takada, M. Ito, Y. Takeoka, Y. Kanda, S. Miyazaki, R. Kuroda, K. Nishida, Pharmacological inhibition of mTORC1 but not mTORC2 protects against human disc cellular apoptosis, senescence, and extracellular matrix catabolism through Akt and autophagy induction, Osteoarthr. Cartil. 27 (6) (2019) 965–976.
[37] K. Nishimura, J. Mochida, Percutaneous reinsertion of the nucleus pulposus, An experimental study, Spine (Phila Pa 1976) 23 (14) (1998) 1531–1538.
[38] M.A. Rousseau, J.A. Ulrich, E.C. Bass, A.G. Rodriguez, J.J. Liu, J.C. Lotz, Stab incision for inducing intervertebral disc degeneration in the rat, Spine 32 (1) (2007) 17–24.
[39] J.H. Jeong, E.S. Jin, J.K. Min, S.R. Jeon, C.S. Park, H.S. Kim, K.H. Choi, Human mesenchymal stem cells implantation into the degenerated coccygeal disc of the rat, Cytotechnology 59 (1) (2009) 55–64.
[40] T. Kawamoto, K. Kawamoto, Preparation of thin frozen sections from nonfixed and undecalcified hard tissues using Kawamot's film method (2012), Methods Mol. Biol. 1130 (2014) 149–164.
[41] K. Ohsawa, Y. Imai, Y. Sasaki, S. Kohsaka, Microglia/macrophage-specific protein Iba1 binds to fimbrin and enhances its actin-bundling activity, J. Neurochem. 88 (4) (2004) 844–856.
[42] D.M. Mosser, J.P. Edwards, Exploring the full spectrum of macrophage activation, Nat. Rev. Immunol. 8 (12) (2008) 958–969.
[43] F.R. Bertani, P. Mozetic, M. Fioramonti, M. Iuliani, G. Ribelli, F. Pantano, D. Santini, G. Tonini, M. Trombetta, L. Businaro, S. Selci, A. Rainer, Classification of M1/M2-polarized human macrophages by label-free hyperspectral reflectance confocal microscopy and multivariate analysis, Sci. Rep. 7 (1) (2017) 8965.
[44] Y. Mori-Akiyama, H. Akiyama, D.H. Rowitch, B. de Crombrugghe, Sox9 is required for determination of the chondrogenic cell lineage in the cranial neural crest, Proc. Natl. Acad. Sci. U.S.A. 100 (16) (2003) 9360–9365.
[45] C. Fang, C.S. Carlson, M.P. Leslie, H. Tulli, E. Stolerman, R. Perris, L. Ni, P.E. Di Cesare, Molecular cloning, sequencing, and tissue and developmental expression of mouse cartilage oligomeric matrix protein (COMP), J. Orthop. Res. 18 (4) (2000) 593–603.
[46] M.E. Joyce, A.B. Roberts, M.B. Sporn, M.E. Bolander, Transforming growth factor-beta and the initiation of chondrogenesis and osteogenesis in the rat femur, J. Cell Biol. 110 (6) (1990) 2195–2207.
[47] Y. Panina, A. Germond, S. Masui, T.M. Watanabe, Validation of common housekeeping genes as reference for qPCR gene expression analysis during iPS reprogramming process, Sci. Rep. 8 (1) (2018) 8716.
[48] K.J. Livak, T.D. Schmittgen, Analysis of relative gene expression data using real-time quantitative PCR and the 2(-Delta Delta C(T)) Method, Methods 25 (4) (2001) 402–408.
[49] K. Masuda, Y. Aota, C. Muehleman, Y. Imai, M. Okuma, E.J. Thonar, G.B. Andersson, H.S. An, A novel rabbit model of mild, reproducible disc degeneration by an anulus needle puncture: correlation between the degree of disc injury and radiological and histological appearances of disc degeneration, Spine 30 (1) (2005) 5–14.
[50] S. Miyazaki, A.D. Diwan, K. Kato, K. Cheng, W.C. Bae, Y. Sun, J. Yamada, C. Muehleman, M.E. Lenz, N. Inoue, R.L. Sah, M. Kawakami, K. Masuda, Issls prize IN basic science 2018: growth differentiation factor-6 attenuated pro-inflammatory molecular changes in the rabbit anular-puncture model and degenerated disc-induced pain generation in the rat xenograft radiculopathy model, Eur. Spine J. 27 (4) (2018) 739–751.
[51] T. Ishikawa, A. Watanabe, H. Kamoda, M. Miyagi, G. Inoue, K. Takahashi, S. Ohtori, Evaluation of lumbar intervertebral disc degeneration using T1rho and T2 magnetic resonance imaging in a rabbit disc injury model, Asian Spine J 12 (2) (2018) 317–324.
[52] S.E. Gullbrand, B.G. Ashinsky, E.D. Bonnevie, D.H. Kim, J.B. Engiles, L.J. Smith, D.M. Elliott, T.P. Schaer, H.E. Smith, R.L. Mauck, Long-term mechanical function and integration of an implanted tissue-engineered intervertebral disc, Sci. Transl. Med. 10 (468) (2018) eaau0670.
[53] D.O. Halloran, S. Grad, M. Stoddart, P. Dockery, M. Alini, A.S. Pandit, An injectable cross-linked scaffold for nucleus pulposus regeneration, Biomaterials 29 (4) (2008) 438–447.
[54] T. Tsujimoto, H. Sudo, M. Todoh, K. Yamada, K. Iwasaki, T. Ohnishi, N. Hirohama, T. Nonoyama, D. Ukeba, K. Ura, Y.M. Ito, N. Iwasaki, An acellular bioresorbable ultra-purified alginate gel promotes intervertebral disc repair: a preclinical proof-of-concept study, EBioMedicine 37 (2018) 521–534.
[55] Y.C. Huang, J.P. Urban, K.D. Luk, Intervertebral disc regeneration: do nutrients lead the way? Nat. Rev. Rheumatol. 10 (9) (2014) 561–566.
[56] K. Gelse, E. Pöschl, T. Aigner, Collagens—structure, function, and biosynthesis, Adv. Drug Deliv. Rev. 55 (12) (2003) 1531–1546.
[57] K.R. Nakazawa, B.A. Walter, D.M. Laudier, D. Krishnamoorthy, G.E. Mosley, K.L. Spiller, J.C. Iatridis, Accumulation and localization of macrophage phenotypes with human intervertebral disc degeneration, Spine J. 18 (2) (2018) 343–356.
[58] T. Takada, K. Nishida, K. Maeno, K. Kakutani, T. Yurube, M. Doita, M. Kurosaka, Intervertebral disc and macrophage interaction induces mechanical hyperalgesia and cytokine production in a herniated disc model in rats, Arthritis Rheum. 64 (8) (2012) 2601–2610.
[59] K. Garg, N.A. Pullen, C.A. Oskeritzian, J.J. Ryan, G.L. Bowlin, Macrophage functional polarization (M1/M2) in response to varying fiber and pore dimensions of electrospun scaffolds, Biomaterials 34 (18) (2013) 4439–4451.
[60] M. Alini, S.M. Eisenstein, K. Ito, C. Little, A.A. Kettler, K. Masuda, J. Melrose, J. Ralphs, I. Stokes, H.J. Wilke, Are animal models useful for studying human disc disorders/degeneration? Eur. Spine J. 17 (1) (2008) 2–19.
[61] M. Bendtsen, C. Bunger, P. Colombier, C. Le Visage, S. Roberts, D. Sakai, J.P. Urban, Biological challenges for regeneration of the degenerated disc using cellular therapies, Acta Orthop. 87 (sup363) (2016) 39–46.